International Journal of Nanomedicine

Dovepress
open access to scientific and medical research

Open Access Full Text Article

ORIGINAL RESEARCH

Autologous serum improves bone formation in a primary stable silica-embedded nanohydroxyapatite bone substitute in combination with mesenchymal stem cells and rhBMP-2 in the sheep model

This article was published in the following Dove Press journal:
International Journal of Nanomedicine
19 November 2014
Number of times this article has been viewed

Anja M Boos[1,*]
Annika Weigand[1,*]
Gloria Deschler[1]
Thomas Gerber[2]
Andreas Arkudas[1]
Ulrich Kneser[1]
Raymund E Horch[1]
Justus P Beier[1]

[1]Department of Plastic and Hand Surgery, University Hospital of Erlangen, Friedrich-Alexander-University of Erlangen-Nürnberg FAU, Erlangen, [2]Institute of Physics, University of Rostock, Rostock, Germany

*These authors contributed equally to this work

Abstract: New therapeutic strategies are required for critical size bone defects, because the gold standard of transplanting autologous bone from an unharmed area of the body often leads to several severe side effects and disadvantages for the patient. For years, tissue engineering approaches have been seeking a stable, axially vascularized transplantable bone replacement suitable for transplantation into the recipient bed with pre-existing insufficient conditions. For this reason, the arteriovenous loop model was developed and various bone substitutes have been vascularized. However, it has not been possible thus far to engineer a primary stable and axially vascularized transplantable bone substitute. For that purpose, a primary stable silica-embedded nanohydroxyapatite (HA) bone substitute in combination with blood, bone marrow, expanded, or directly retransplanted mesenchymal stem cells, recombinant human bone morphogenetic protein 2 (rhBMP-2), and different carrier materials (fibrin, cell culture medium, autologous serum) was tested subcutaneously for 4 or 12 weeks in the sheep model. Autologous serum lead to an early matrix change during degradation of the bone substitute and formation of new bone tissue. The best results were achieved in the group combining mesenchymal stem cells expanded with 60 µg/mL rhBMP-2 in autologous serum. Better ingrowth of fibrovascular tissue could be detected in the autologous serum group compared with the control (fibrin). Osteoclastic activity indicating an active bone remodeling process was observed after 4 weeks, particularly in the group with autologous serum and after 12 weeks in every experimental group. This study clearly demonstrates the positive effects of autologous serum in combination with mesenchymal stem cells and rhBMP-2 on bone formation in a primary stable silica-embedded nano-HA bone grafting material in the sheep model. In further experiments, the results will be transferred to the sheep arteriovenous loop model in order to engineer an axially vascularized primary stable bone replacement in clinically relevant size for free transplantation.

Keywords: nanostructured bone substitute, bone tissue engineering, autologous serum, mesenchymal stem cells, recombinant human bone morphogenetic protein 2, sheep model

Introduction

Critical size bone defects are still an unsolved problem in orthopedic and reconstructive surgery. Autologous bone grafts are the most common treatment used for defects resulting from tumor excision, debridement after osteomyelitis, or crush injuries, and are the gold standard of current therapeutic strategies. Donor site morbidities are a well known but unsolved problem after autologous bone graft harvesting. Tissue engineering came into the focus of researchers many years ago for the improvement of treatment concepts and also for studying cellular interactions.[1,2] In the interdisciplinary field of

Correspondence: Anja M Boos
Department of Plastic and Hand Surgery, University Hospital of Erlangen, Friedrich-Alexander-University of Erlangen-Nürnberg Krankenhausstrasse 12, D-91054 Erlangen, Germany
Tel +49 913 1853 3277
Fax +49 913 1853 9327
Email anja.boos@uk-erlangen.de

bone tissue engineering, a large number of studies[3,4] were published on restoring a defect with the aid of biomaterials, cells, and signal molecules.

Optimal bone scaffolds possess osteogenic potential, provide shape for a certain period, and subsequently degrade easily within the biological environment.[5] Within the broad range of biomaterials, calcium phosphate-based bioceramics, especially hydroxyapatite (HA), β-tricalcium phosphate, bioglasses, and mixtures thereof, are most widely used and considered to be biocompatible, non-immunogenic, and osteoconductive.[6,7]

Several studies were able to demonstrate the benefit of early bone ingrowth and repair through the incorporation of silicon into porous HA or calcium silicate ceramics.[8,9,13,31] Others investigated the influence of silicon on cell proliferation and osteogenic signaling in human mesenchymal stem cells (MSC) and could show transient osteogenic signals in MSC.[10,11]

A silica gel-embedded, non-sintered nanocrystalline HA bone substitute (NanoBone®; Artoss GmbH, Rostock, Germany) with interconnecting pores from nanometer to millimeter range was recently developed and approved.[12] It was evaluated in several experimental studies as demonstrating faster bone formation, remodeling, and resorption rates after implantation, compared with other commercially available HA, tricalcium phosphate, or gelatin sponge materials.[13–15]

For further osteoinductive effects, the utilization of osteogenic cells, such as mature osteoblasts or multipotent MSC isolated from bone marrow, trabecular bone, adipose tissue, synovial membrane, or other tissue types, is an established strategy in bone tissue engineering.[16–19] The application of MSC was investigated for bone tissue engineering purposes and appeared to be superior to other cell types in terms of osteogenic differentiation capacity and osteoinductive properties.[5]

One possibility for improving the osteoinductivity of scaffolds is the application of biologically active molecules. Growth factors that occur within a healthy bone matrix or are expressed during fracture healing are, for example, transforming growth factor β, insulin-like growth factor I and II, platelet-derived growth factor, fibroblast growth factor, and various types of bone morphogenetic proteins (BMPs). BMPs are members of the transforming growth factor β superfamily and are well known to be osteoconductive and chondroinductive.[20,21] However, the clinical application of BMPs is restricted to limited indications, for example, in non-unions and spinal fusion.[22]

The sheep arteriovenous loop model was established in recent years to engineer vascularized transplantable tissues in clinically relevant size. Bone matrices were vascularized and ectopic bone parts were engineered. However, a bone block that was stable enough for transplantation in a critical size bone defect has thus far not been generated. The present study aimed to evaluate a primary stable nanocrystalline HA bone substitute material and a suitable cell source in combination with recombinant human (rh)BMP-2 and different carrier materials to engineer a bone block with sufficient primary stability.

After engineering a stable bone block in the subcutaneous model, the results should be evaluated in the arteriovenous loop model with the view to axially vascularized tissue engineering and free transplantable primary stable bone replacement.

Materials and methods

Sheep model and operative technique

In total, eleven female merino land sheep with a body weight of 25–35 kg, aged 4–5 months, were operated on. German regulations for the care and use of laboratory animals were observed at all times. The Animal Care Committee of the University of Erlangen-Nürnberg and the government of Mittelfranken, Germany, approved all experiments (Az 54.2531.31-23/06/Az 54-2532.1-44/11). The animals were housed in the veterinary care facility under standardized conditions of 55% air humidity and 18°C room temperature with a 12-hour light/dark rhythm as described previously.[23] The sheep were fed once a day with a standard sheep diet (ssniff-Spezialdiäten GmbH, Soest, Germany) and hay and water ad libitum. The animals were deprived of food for 24 hours prior to surgery to limit regurgitation.

Sedation and analgesia of the sheep were induced by administration of midazolam (Midazolam-ratiopharm®; ratiopharm GmbH, Ulm, Germany) 0.5–1 mg/kg intramuscularly and ketamine 5–10 mg/kg intramuscularly (Ketavet®; Pharmacia GmbH, Berlin, Germany). Subsequently, orotracheal intubation (7.5 Charrière) was performed under laryngoscopic control. The respirator (Dräger, Lübeck, Germany) was adjusted to controlled artificial respiration using intermittent positive pressure ventilation with weight-adapted breath volume. Anesthesia was maintained by inhalation of a gas mixture of 1%–2% isoflurane (Forene®; Abbott GmbH & Co., KG, Wiesbaden, Germany) with air/oxygen. To adjust intraoperative fluid volume loss, the animals received weight-adapted crystalloids (Fresenius

Kabi AG, Bad Homburg, Germany) during the operation. Perioperative antibiotic therapy (1–1.25 mg/kg cefquinome; Cobactan®; Intervet Deutschland GmbH, Unterschleißheim, Germany) was administered intramuscularly, followed by a postoperative administration. Carprofen 4 mg/kg was given subcutaneously (Rimadyl®; Pfizer, Berlin, Germany) as postoperative analgesia.

The surgical site was shaved, prepped, and draped for sterility. Subcutaneous pockets were prepared on the back of the sheep. Two nano-HA bone substitute blocks were sutured together with a non-absorbable 3-0 suture, resulting in a diameter of 15×10×10 mm and a volume of 1.5 cm^3 per construct. Scaffolds were implanted into the subcutaneous pockets, which were closed with non-absorbable 2-0 interrupted sutures.

In the first part of the study, bone substitute blocks (Artoss GmbH) were soaked with different carrier materials (fibrin fibrinogen-thrombin-matrix TISSEEL - Fibrin Sealant, Baxter Healthcare SA, Zurich, Switzerland], Dulbecco's Modified Eagle's Medium [Gibco/Life Technologies, Carlsbad, CA, USA], autologous serum) in combination with expanded and directly retransplanted MSC for an implantation period of 4 weeks (n=2). The MSC were loaded by a vacuum procedure into the scaffolds.

Fibrin was prepared according to the manufacturer's protocol. In brief, sealer protein concentrate was dissolved in aprotinin solution (3,000 KIU/mL). Fibrinogen was diluted to a concentration of 20 mg/mL by addition of fibrinogen buffer. Next, 5 mL of 40 mM $CaCl_2$ solution was added to thrombin for a final concentration of 500 IU/mL. Blood was collected by puncture of the jugular vein using serum S-Monovette® needles (Sarstedt AG & Co, Nümbrecht, Germany). After clotting, serum was obtained by centrifugation (10 minutes, 3,400 g).

In the second part of the study, bone substitute block was soaked with 2 mL blood, 2 mL bone marrow, or expanded or directly retransplanted MSC, and 60 µg/mL rhBMP-2 (InductOs®; Wyeth Pharmaceuticals, Pfizer Inc., New York City, NY, USA) dissolved in 1.5 mL of the carrier material, depending on the experimental group. The constructs were implanted for 12 weeks (n=5; Figure 5A and B).

In the third part of the study, the best groups in parts 1 and 2 were combined and implanted for 12 weeks (n=5). Bone substitute blocks with fibrin (1.5 mL) were used as the control. An overview of the groups is given in Table 1. All constructs were distributed over different animals. In the second and third parts of the study, it was determined that the control group fibrin was implanted in each sheep.

For explanting of constructs, the sheep were anesthetized as described above. Euthanasia was performed using T61® indepth anesthesia (5–10 mL/50 kg intravenously; Intervet International GmbH).

Table 1 Overview of the different experimental groups

Implantation time period (weeks)	Bone substitute	Cell carrier material	Mesenchymal stem cells	rhBMP-2
Study part one				
4	NanoBone® n=2	Fibrin	Directly retransplanted	–
4		Fibrin	Expanded	–
4		Cell culture medium	Directly retransplanted	–
4		Cell culture medium	Expanded	–
4		Autologous serum	Directly retransplanted	–
4		Autologous serum	Expanded	–
Study part two				
12	NanoBone® n=5	Fibrin	–	–
12		Bone marrow	–	–
12		Blood	–	–
12		Fibrin	Directly retransplanted	–
12		Fibrin	Expanded	–
12		Fibrin	–	60 µg/mL
Study part three				
12	NanoBone® n=5	Fibrin	Expanded	60 µg/mL
12		Autologous serum	Expanded	60 µg/mL

Notes: For evaluation of optimal carrier materials, the bone substitute block was soaked with fibrin, cell culture medium, or autologous serum, and implanted subcutaneously in sheep for 4 weeks (part 1 of the study). Additional implantation of different cells and the bone growth factor rhBMP-2 were evaluated in a 12-week group (part 2 of the study). In part 3 of the study, the best experimental groups from the first two parts were combined.
Abbreviation: rhBMP-2, recombinant human bone morphogenetic protein 2.

Bone marrow harvesting, and isolation and cultivation of MSC

After sedation and analgesia of the sheep and local anesthesia (prilocaine hydrochloride, Xylonest® 1%; AstraZeneca, London, UK), a small incision was made above the spina iliaca dorsalis cranialis (human anatomical correlate: posterior superior iliac spine) of the iliac crest. An 11 gauge needle was used to puncture the iliac crest and about 20 mL of bone marrow were aspirated into heparin-coated syringes (6,000 IE/10 mL). The bone marrow was diluted with phosphate-buffered saline 1:4 (Dulbecco 1×; Biochrom AG, Berlin, Germany) and bone marrow stem cells were harvested by Ficoll gradient centrifugation as described previously.[23]

MSC were immediately retransplanted without any interim expansion or storage procedure, or expanded in Dulbecco's Modified Eagle's Medium with 1% penicillin-streptomycin and 10% fetal calf serum (all from Biochrom AG) to a final cell number of 6 million per implant. Before implantation, the cells were labeled using dioctadecyl-3,3,3′3′-tetramethylindocarbocyanine perchlorate; CellTracker™ CM-DiI, (Invitrogen, Carlsbad, CA, USA) according to the manufacturer's protocol.

Histomorphometric analyses

For histomorphometric analyses, the cross-sectional areas of the specimens, degraded bone substitute, area with tissue ingrowth, and newly formed bone were measured and calculated as follows. After explantation, constructs were formalin-fixed, decalcified by EDTA (ethylenediaminetetraacetic acid) solution (Fluka; Sigma-Aldrich Corporation, St Louis, MO, USA) in an ultrasonic bath (Sonocool® 255; Bandelin GmbH & Co., KG, Berlin, Germany), and paraffin-embedded. Next, 3 µm cross-sections were obtained from two standardized planes using a rotary microtome (Microm International GmbH, Walldorf, Germany). Paraffin sections were stained with hematoxylin-eosin and photomicrographs were taken using a Leica microscope and digital camera (Leica Microsystems, Wetzlar, Germany).

For histomorphometric analyses, two sections per specimen were completely scanned at 25× magnification and merged into one image (Adobe Photoshop CS3 extended; Adobe Systems Inc., San Jose, CA, USA). This image was analyzed semiautomatically in the Leica Application Suite V3 according to the user's manual. One blinded observer detected typical coloring in the hematoxylin-eosin staining for measuring bone surface, cross-sectional and bone substitute degradation area, or in the periodic acid Schiff (PAS) staining for calculation of tissue ingrowth area. Images were further processed by generating binary images. These program settings were used for all images. Areas were calculated automatically by the program. Mean values for the results of both planes were used for statistical analyses.

For calculating absorption of the whole specimen, the cross-sectional area was measured and correlated with the cross-sectional area of a bone substitute block before implantation (bone substitute native). Degraded bone substitute was calculated using the bone substitute and pore surface of a native bone substitute block.

In the second and third parts of the study, the impact of the different bone formation potential of sheep was reduced by back calculating the percentage of newly formed bone area in the experimental group to the percentage of newly formed bone area in the control group (bone substitute with fibrin).

For the detection of bone remodeling processes, histochemical tartrate-resistant acidic phosphatase (TRAP) staining was used to identify TRAP-positive, osteoclast-like cells. After deparaffinization and rehydration, the slides were incubated in TRAP buffer (pH 5) containing 3.28 g/L sodium acetate (Merck KGaA, Darmstadt, Germany) and 46.01 g/L sodium tartrate dehydrate (Carl Roth GmbH & Co., KG, Karlsruhe, Germany) for 10 minutes. Immediately afterwards, the sections were placed in freshly prepared TRAP staining solution consisting of 10 mg naphthol AS-MX phosphate and 60 mg Fast Red Violet LB Salt (both Sigma-Aldrich Chemie GmbH, Steinheim, Germany), 1,000 µL N-N-dimethylformamide (Merck KGaA), 500 µL Triton X-100 (Carl Roth GmbH & Co. KG), and 50 mL TRAP buffer. After an incubation period of about 10–60 minutes at 37°C, this reaction was stopped by a washing step in distilled water. TRAP-positive cells developed red staining. Finally, the slides were counterstained with Mayer's hemalaun solution (Merck KGaA).

To determine the extent of osteoclastic activity, four regions of interest were examined at 200× magnification in two planes for each specimen. Regions of interest were chosen at each of the center points of the four outer sides, always ensuring that regions of interest were located in an area of tissue ingrowth. To distinguish TRAP-positive osteoclasts from other cells, such as tissue macrophages and foreign body giant cells, osteoclasts had to meet the following criteria: proximity to bone/bone substitute, more than two nuclei, ruffled border, and granular cytoplasm. For calculation of the osteoclast density per micrometer bone substitute,

TRAP-positive cells and length of bone substitute per region of interest were measured (using the interactive measurement of the Leica Application Suite, Leica Microsystems).

Immunohistochemical staining

For identification of endothelial cells, immunohistochemistry with a von Willebrand factor antibody (polyclonal rabbit anti-human/mouse/rat; Biocare Medical, Concord, NH, USA) and a secondary biotinylated antibody (anti-rabbit IgG [H+L]; Vector Laboratories Inc., Burlingame, CA, USA) was performed by means of the ABC reagent (Vectastain® Elite ABC Reagent RTU; Vector Laboratories Inc).

Endothelial cells were also detected by CD31 immunofluorescence staining with a primary monoclonal mouse anti-ovine CD31 antibody (Anti-CD31/PECAM-1; MorphoSys AG, Martinsried/Planegg, Germany) using a biotin-free tyramide signal amplification system (CSA II system; Dako Denmark A/S, Glostrup, Denmark).

Both endothelial cell stainings were performed, because of the better histological overview in the von Willebrand factor staining and the increased possibility of locating DiI-labeled MSC in relation to the blood endothelial cells in the CD31 staining. Using the same system, Ki67 (mouse anti-human Ki67 clone MIB-1; DakoCytomation A/S, Glostrup, Denmark) immunofluorescence staining was performed to determine cell proliferation.

For detection of apoptotic cells, a terminal deoxynucleotidyl transferase dUTP nick end labeling (TUNEL) assay (fluorescein FragEL™ DNA fragmentation detection kit; Calbiochem/Merck KGaA) was used.

Collagen type I immunohistochemical staining with a primary antibody against collagen type I (polyclonal rabbit anti-bovine antibody; Biologo, Kronshagen, Germany) and a biotinylated secondary antibody (anti-rabbit IgG [H+L]; Vector Laboratories Inc) was performed using the ABC reagent for detection of bone area.

Osteoblasts were visualized with an alkaline phosphatase (not tissue-specific) polyclonal rabbit anti-human antibody (GeneTex Inc., Irvine, CA, USA) using the DakoCytomation EnVision® + Dual Link System-HRP (DAB+; Dako Denmark A/S).

For visualization of the matrix change of the bone substitute from an inorganic into an organic matrix, PAS staining was performed. Slides were incubated for 5 minutes in periodic acid which oxidizes glycols into aldehydes. Thereafter, staining was performed with Schiff reagent for 15 minutes under formation of a purple dye (PAS staining kit, Carl Roth GmbH & Co., KG).

An antibody against alpha smooth muscle cells (αSMA) was used for determination of vessel maturation (clone 1A4). Using a ZytoChemPlus (AP) polymer bulk kit (both from Zytomed Systems GmbH, Berlin, Germany), αSMA-positive cells were stained in red color.

Counterstaining was always performed with Mayer's hemalaun solution (Merck KGaA) or, in the case of immunofluorescence staining, with 4′,6-diamidino-2′-phenylindole dihydiochloride (DAPI; Roche Applied Science/Roche, Basel, Switzerland).

Scanning electron microscopy and energy dispersive x-ray spectroscopy

For characterization of the material architecture, composition, and matrix change of the bone substitute block, scanning electron microscopy and energy dispersive x-ray spectroscopy analyses were performed for a range of decalcified slides in each experimental group (DSM 960 scanning electron microscope with a silicon detector; Carl Zeiss AG, Oberkochen, Germany, using software by SAMx, Lavardens, France).

Quantitative real-time PCR

For RNA isolation, one part of each construct was dissected and immediately frozen in liquid nitrogen. Constructs were powdered using a Mixer Mill MM200 (Retsch GmbH, Haan, Germany). TRIzol® reagent (Ambion, Life Technologies), chloroform (Th Geyer GmbH & Co., KG, Renningen, Germany) and ethanol (Merck KGaA) were added to the powder to isolate RNA according to the phenol chloroform extraction protocol. In addition, RNA purification was performed using a RNeasy mini kit (Qiagen, Hilden, Germany). The probes were reverse-transcribed into complementary DNA using an Omniscript® reverse transcription kit, oligo-dT primers, and RNase inhibitor (Qiagen). Quantitative real-time polymerase chain reaction (PCR) was carried out using ABsolute™ qPCR SYBR® Green Mix (Thermo Fisher Scientific, Waltham, MA, USA) and a Light Cycler (iCycler iQ5; Bio-Rad Laboratories Inc., Hercules, CA, USA). All kits were used according to the manufacturers' protocols. Samples were tested as triplicates, and only variations of less than 1.5 threshold cycles were tolerated. Threshold cycles after cycle 35 were defined as invalid. Data evaluation was performed using the $\Delta\Delta C_T$-method.

Real-time PCR was performed to assess the upregulation of genes important for osteogenesis, such as collagen I (forward primer ′AAGACATCCCACCAGTCACC′; reverse primer ′TAAGTTCGTCGCAGATCACG′), osteocalcin (forward primer ′TGAGCTCAACCCTGACTGTG′; reverse primer

′GTCCTGGAGAGAAGCCAGAG′), osteonectin (forward primer ′ACGGGTACCTGTCTCACACC′; reverse primer ′GTCCAGGGCGATGTACTTGT′) osteopontin (forward primer ′TCCCACTGACATTCCAACAA′; reverse primer ′CTGTGGCATCTGGACTCTCA′) and RUNX2 (forward primer ′CGCATTCCTCATCCCAGTAT′; reverse primer ′GCCTGGGGTCTGTAATCTGA′) within the constructs. Actin (forward primer ′GTCCACCTTCCAGCAGATGT′; reverse primer ′ATCTCGTTTTCTGCGCAAGT′) was used as the housekeeping gene.

Statistical analysis

The data are expressed as the mean ± standard deviation. The statistical analysis was performed using Statistical Package for the Social Sciences version 18.0 for Windows (IBM Corporation, Armonk, NY, USA). Results of these histomorphometric and molecular biological analyses were interpreted statistically by one-way analysis of variance and Tukey's honest significant difference test as a post hoc test. Due to the small group size, a normal distribution was confirmed using the Shapiro–Wilk test. The assumption of sphericity was tested by Mauchly's test of sphericity. However, also in the case of non-violation, Greenhouse-Geisser correctional adjustment was applied due to the small group size. In the event of a non-normal distribution, the non-parametric Kruskal–Wallis test was used together with the Mann–Whitney *U*-test with a Bonferroni-corrected significance level ($\alpha' = \alpha/m$, where α is the level of significance and m is the number of comparisons). For comparing two samples, the Student's *t*-test for independent samples was used. Homogeneity of variance was checked using Levene's test. Non-normally distributed samples were tested by the non-parametric Mann–Whitney *U*-test. The level of statistical significance was set to $P \leq 0.05$. A *P*-value ≤ 0.01 was considered to be highly statistically significant. In part 1 of the study, no statistical tests were used due to the small sample size.

Results

Part 1 of the study was carried out for evaluation of the best carrier material (fibrin, cell culture medium, autologous serum) for cells or growth factors to be used in implantation of the nanostructured bone substitute block. In part 2, the scaffold was implanted with different cells (bone marrow, blood, expanded and directly retransplanted MSC) and with the growth factor rhBMP-2. In part 3 of the study, the most promising groups (autologous serum, expanded MSC, rhBMP-2) were combined in two booster groups (expanded MSC and rhBMP-2 in autologous serum and additionally in fibrin; the experimental groups are shown in Table 1).

Biocompatibility of nanostructured bone substitute material

In total, 14 separate experimental groups were evaluated in the sheep model. Postoperative seroma at the implantation site developed in a few of the sheep. One of the sheep in the fibrin group developed an infection. Infection did not occur in the blood or bone marrow group (data not shown). This sheep with infected implants was excluded from the study and the groups were repeated in another sheep. None of the other sheep showed any signs of infection or intolerance of the implants. No invasion of inflammatory cells as a sign of immune response was obvious in the explants (Figures 1A and 6A).

Evaluation of different carrier materials

To enhance perfusion of the bone substitute with cells and growth factors and to support early cell ingrowth and invasion of vasculature, we decided to compare different carrier materials. Cell culture medium and autologous serum were used instead of fibrin and compared with respect to

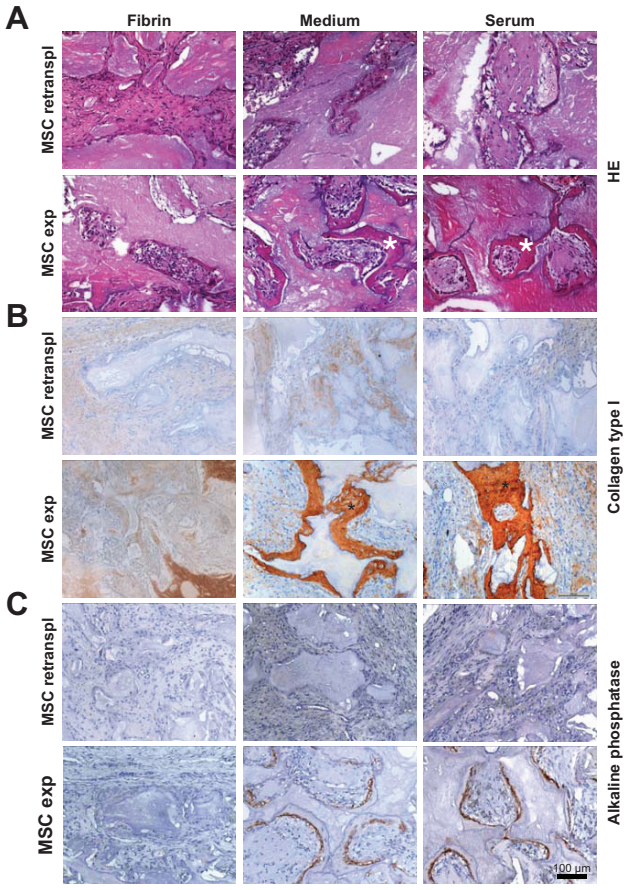

Figure 1 Hematoxylin-eosin (**A**), collagen type I (**B**), and alkaline phosphatase (**C**) immunohistochemical staining in the 4-week group. Bone formation was only seen in the groups with MSC expanded in autologous serum or cell culture medium (*).
Abbreviations: exp, expanded; retranspl, retransplanted; HE, hematoxylin-eosin; MSC, mesenchymal stem cells.

handling, tissue ingrowth, cross-sectional areas of the whole construct, degraded bone substitute area, vascularization, bone formation, and cell behavior. Groups were implanted, comparing all three carrier materials with directly retransplanted and expanded MSC.

Hematoxylin-eosin and immunohistochemical staining against collagen type I and alkaline phosphatase demonstrated bone formation after 4 weeks only in the experimental groups with expanded MSC in cell culture medium or autologous serum (Figure 1A–C).

Considerably more bone was seen in constructs with expanded MSC soaked with cell culture medium or autologous serum, compared with fibrin (Figure 2A). Quantitative real-time PCR analyses revealed upregulation of the bone-specific genes, osteonectin, osteopontin, collagen type I, and RUNX2 in all groups, compared with the control (Figure 2D). Bone substitute degradation in fibrin was about 20%. In cell culture medium and autologous serum with expanded MSC, bone substitute particles were degraded to a higher extent of about 40% (Figure 2B).

In constructs soaked in cell culture medium and autologous serum with expanded MSC, a higher level of tissue ingrowth was seen when compared with fibrin (Figure 2C). In some sections, only the original bone substitute particles

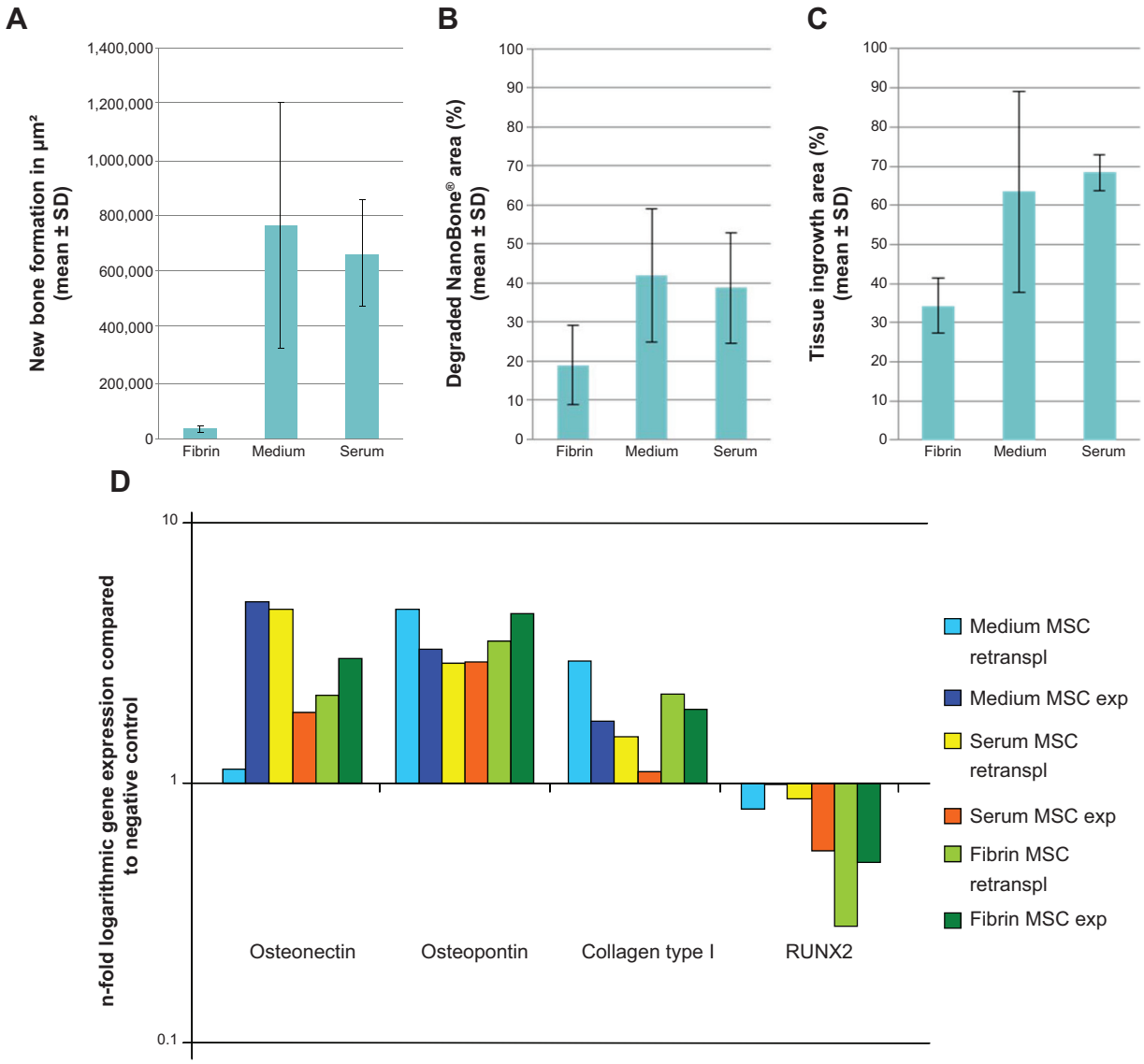

Figure 2 New bone formation, degradation of NanoBone® and tissue ingrowth.
Notes: (**A**) Significantly more bone was seen in constructs with expanded MSC soaked with autologous serum and cell culture medium compared with the fibrin group. (**B**) Bone substitute degradation in fibrin was about 20%, in medium and autologous serum with expanded MSC, and bone substitute particles were degraded to a higher extent of about 40%. (**C**) All constructs were analyzed for tissue ingrowth by periodic acid Schiff staining. In constructs with expanded MSC soaked with medium and autologous serum, a higher level of tissue ingrowth and vascularization was seen compared with the fibrin group. (**D**) Quantitative real-time polymerase chain reaction analyses revealed upregulation of the bone-specific genes, osteonectin, osteopontin, collagen type I, and RUNX2, in all groups compared with the control (fibrin group).
Abbreviations: exp, expanded; retranspl, retransplanted; MSC, mesenchymal stem cells; SD, standard deviation.

without any surrounding tissue could be detected. Less tissue ingrowth was shown in the 4-week compared with the 12-week group (data not shown).

Staining against von Willebrand factor and CD31 revealed a dense vascular network in the areas with tissue ingrowth (Figure 3A and B). DiI-labeled cells could be detected in all explants, but to a lesser extent in the group with directly retransplanted MSC (Figure 3B and C). Ki67 staining demonstrated proliferation of cells in all constructs to a comparable extent (Figure 3C).

In all constructs, osteoclastic activity was observed by TRAP staining. However, more TRAP-positive cells could be detected in the experimental groups with cell culture medium or autologous serum and expanded MSC, in comparison with fibrin (Figure 4A and B). Fewer TRAP-positive cells were seen in the serum group after 4 weeks than after 12 weeks (Figure 4C).

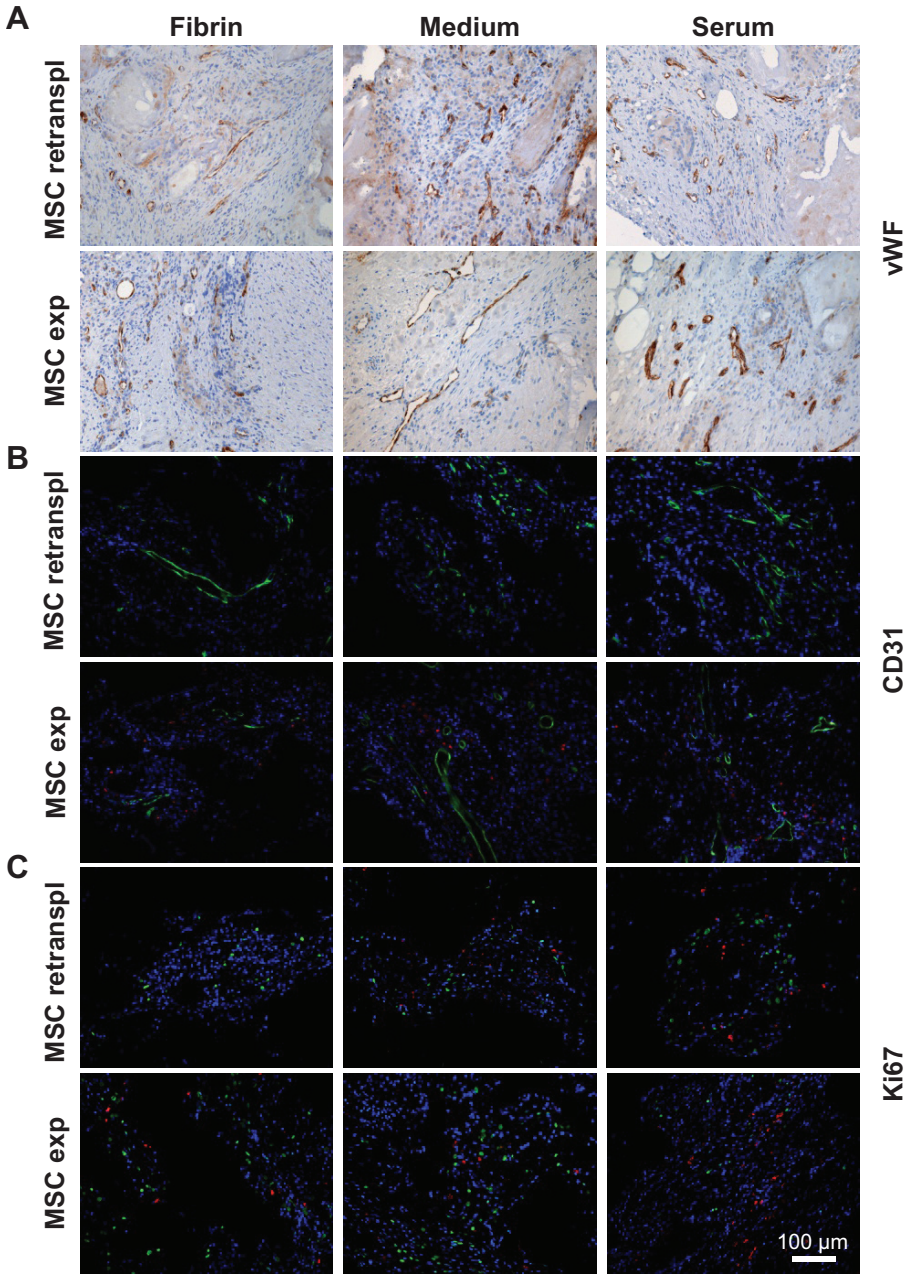

Figure 3 Vascularization of the explants and cell proliferation.
Notes: Staining against vWF (brown) (**A**) and CD31 (green) (**B**) of sections in the 4-week group revealed a dense vascular network nearly all over the explants. For retrieval of implanted MSC, the cells were labeled using DiI (red staining) before implantation. DiI-labeled cells could be detected mainly in the groups with expanded MSC. (**C**) To establish viability and active proliferation of the transplanted cells, Ki67 (green) staining was performed, demonstrating proliferation of cells in all constructs to a comparable extent.
Abbreviations: exp, expanded; retranspl, retransplanted; MSC, mesenchymal stem cells; vWF, von Willebrand factor; DiI, dioctadecyl-3,3,3′3′-tetramethylindocarbocyanine perchlorate.

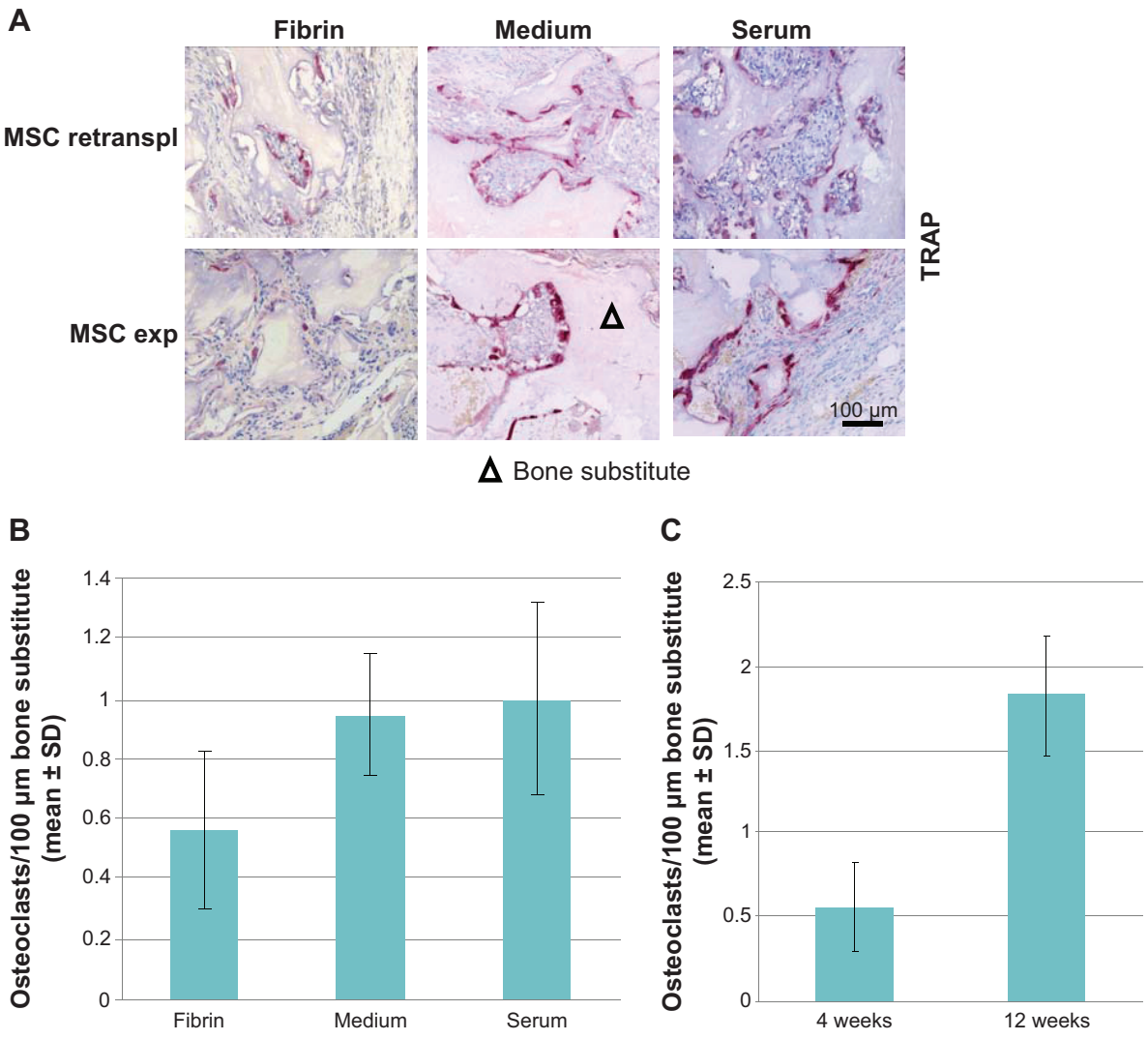

Figure 4 Osteoclastic activity in the explants.
Notes: (**A**) Sections of all experimental groups were stained for TRAP to assess osteoclastic activity. Osteoclasts (stained in red) are visible mainly on the surface of the bone substitute particles. (**B**) Osteoclastic activity was observed in all constructs by TRAP staining. However, more TRAP-positive cells could be detected in the experimental groups with expanded MSC in autologous serum and cell culture medium, in comparison with fibrin. (**C**) After 4 weeks, fewer TRAP-positive cells were seen in the serum group with expanded MSC than after 12 weeks in the group with expanded MSC and rhBMP-2 in serum.
Abbreviations: exp, expanded; retranspl, retransplanted; MSC, mesenchymal stem cells; SD, standard deviation; TRAP, tartrate-resistant acidic phosphatase; rhBMP-2, recombinant human bone morphogenetic protein 2.

Composition of the explants

Different explant volumes were evident between the different groups. The explants from the blood and bone marrow group seemed to shrink more, resulting in volumes about half those of the explants from the other groups (Figure 5C and D). In the measurement of cross-sectional area correlated to a bone substitute block before implantation (bone substitute native), the smallest cross-sectional areas were encountered in explants from the blood and bone marrow group. All the other groups showed a 30%–40% smaller area and a highly significant reduction when compared with bone substitute native.

The blood and bone marrow explants had a significantly or highly significantly smaller cross-sectional area than explants in the fibrin group (P=0.004 compared with bone marrow; P=0.011 compared with blood), rhBMP-2 group (P=0.036 compared with bone marrow), expanded MSC group (P=0.005 compared with bone marrow; P=0.014 compared with blood), or the group consisting of expanded MSC in combination with rhBMP-2 in serum (P=0.004 compared with bone marrow; P=0.01 compared with blood; Figure 5G).

In addition, degradation of bone substitute was calculated. All explants showed about 40%–50% less bone substitute content when compared with bone substitute native (Figure 5H). There was no significant difference between the groups.

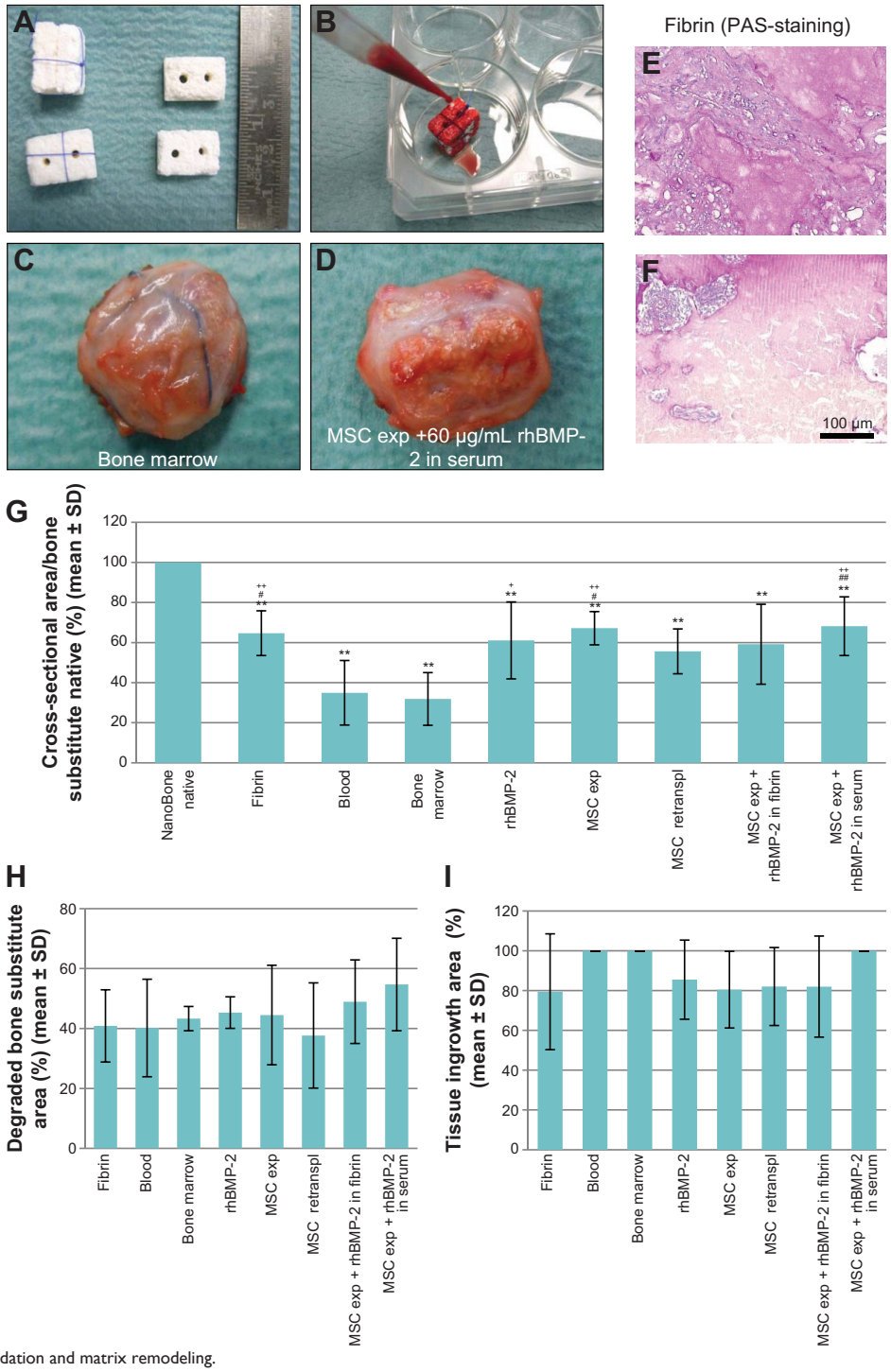

Figure 5 Explant degradation and matrix remodeling.

Notes: (**A**) For each implant, two bone substitute blocks were sutured together to achieve a construct size of about 1.5 cm³. (**B**) This image depicts the soaking procedure from one implant with blood. (**C** and **D**) Different construct volumes were obvious during explantation between the different groups. Explants in the blood and bone marrow group shrank more than the other explants, measuring about half of the volume of explants from the other experimental groups. Explants from the bone marrow group and from the group with expanded MSC and rhBMP-2 in autologous serum are shown as examples. (**E**, **F**, **I**) All constructs were analyzed for tissue ingrowth by PAS staining. The area was then measured semiautomatically. In all explants, tissue ingrowth was about 80%–100% of the whole construct. In the blood, bone marrow, and autologous serum group, optimal tissue ingrowth of 100% was observed. (**G**) For quantification of shrinkage of the constructs during the implantation period, cross-sectional areas of the whole explants were measured and correlated with a bone substitute block before implantation (bone substitute native). In explants from the blood and bone marrow group, significantly and highly significantly smaller cross-sectional areas were noticed compared with other experimental groups; 30%–40% fewer cross-sectional areas were observed in all other groups compared with the bone substitute native. (**H**) Degradation of the bone substitute was calculated. All explants showed about 40%–50% less bone substitute content compared with bone substitute native. There was no significant difference between the groups. *$P \leq 0.05$ significant versus bone substitute native; #significant versus blood; +significant versus bone marrow, **$P \leq 0.01$ highly significant versus bone substitute native; ##highly significant versus blood; ++highly significant versus bone marrow.

Abbreviations: exp, expanded; retranspl, retransplanted; MSC, mesenchymal stem cells; PAS, periodic acid Schiff; SD, standard deviation; rhBMP-2, recombinant human bone morphogenetic protein 2.

Tissue ingrowth

Slides were stained for PAS (Figure 5E and F) and the area of tissue ingrowth was measured semiautomatically. The shift from an inorganic to an organic matrix could be demonstrated in all areas where tissue had grown. The surfaces of the bone substitute particles, which were surrounded by newly formed tissue, were purple in color, indicating a high content of polysaccharides, neutral mucopolysaccharides, mucoglycoproteins, and glycoproteins, as well as glycolipids and phospholipids (Figure 5E). In contrast, areas with no tissue ingrowth showed weaker staining and could be distinguished very well (Figure 5F).

All explanted constructs showed tissue ingrowth areas of about 80%–100%. Especially in the border parts of the explants, nano-HA bone substitute particles were surrounded by connective tissue and blood vessels. In the center of some constructs, there was partly no tissue ingrowth on the overview pictures. The explants from the blood, bone marrow, and autologous serum group seemed to have the best tissue ingrowth of 100%. There were no statistically significant differences between the groups (Figure 5I).

Bone formation

For detection of newly formed bone tissue, slides of all experimental groups were stained against collagen type I, the main component of the organic bone matrix, and alkaline phosphatase, an enzyme synthesized by osteoblasts. Areas positive for collagen type I and alkaline phosphatase could be detected above all in the groups with expanded MSC and rh-BMP-2 in combination with fibrin and serum, as well as in the rhBMP-2 group. Newly formed bone parts could be seen particularly on the surfaces of bone substitute particles. Alkaline phosphatase could be detected near the ossification zone next to osteoblasts synthesizing new bone tissue (Figure 6B and C).

New bone formation was quantified semiautomatically as mentioned in the Material and methods section (Figure 7A and B). In the booster groups, combining rhBMP-2 and expanded MSC in carrier medium fibrin or autologous serum, the highest quantities of bone formation could be achieved (Figure 7C). Subcutaneous bone substitute implants with two different concentrations of rhBMP-2 (12 and 60 µg/mL) have been evaluated in previous experiments, and shown the 60 µg/mL concentration to be superior (data not shown). Comparing the two booster groups, in the group combining rhBMP-2 and expanded MSC in autologous serum, significantly more bone formation could be achieved (P=0.025; Figure 7D). Expanded MSC and rhBMP-2 alone could enhance bone formation, but, in combination with autologous serum, bone formation was significantly higher (P=0.016; Figure 7E). Quantitative real-time PCR analyses revealed upregulation of the bone-specific markers, osteocalcin, osteonectin, osteopontin, collagen type I and RUNX2, in nearly all groups when compared with the control (fibrin; Figure 7F). There were no statistically significant differences between the groups.

Osteoclastic activity

Slides of all experimental groups were TRAP-stained for quantitative evaluation of osteoclastic activity. Osteoclasts were mainly located at the surface of the bone substitute particles, showing a nearly equal distribution of osteoclastic activity over the constructs. Osteoclasts were counted semiautomatically as mentioned in the Material and methods section. There were no significant differences between the experimental groups (Figure 8A and B).

Matrix change

Scanning electron microscopy and energy dispersive x-ray spectroscopy analyses were performed from slides of each experimental group to confirm the element composition in the constructs. For these measurements, two to eight different positions were chosen per section concerning structure and shading. In areas with no or slight tissue ingrowth, relatively high levels of silicon and oxygen could be detected, reflecting the original composition of the bone substitute particles (Figure 9A, position 1). However, in areas with high tissue ingrowth, high carbon and low silicon levels were found, indicating the change from an inorganic to an organic matrix (Figure 9A, position 2). In Figure 9B–E, different magnifications of the histological sections are shown. The matrix change could be observed particularly in the border parts of the constructs, in contrast with the centrally located areas with no tissue ingrowth.

Vascularization of constructs

To examine vascularization, sections from each experimental group were stained against CD31, von Willebrand factor, and αSMA. Newly formed vessels could be detected and were nearly equally distributed all over the constructs in areas with tissue ingrowth. In general, the endothelial cell layer of the vessels could be nicely stained for CD31 and von Willebrand factor, showing different sizes of vessels in the construct. In addition, maturation of larger vessels by coverage of smooth muscle cells was shown by αSMA staining. Remodeling of the vascularization of the constructs in a hierarchically organized system could be demonstrated by the staining (Figure 10A–C).

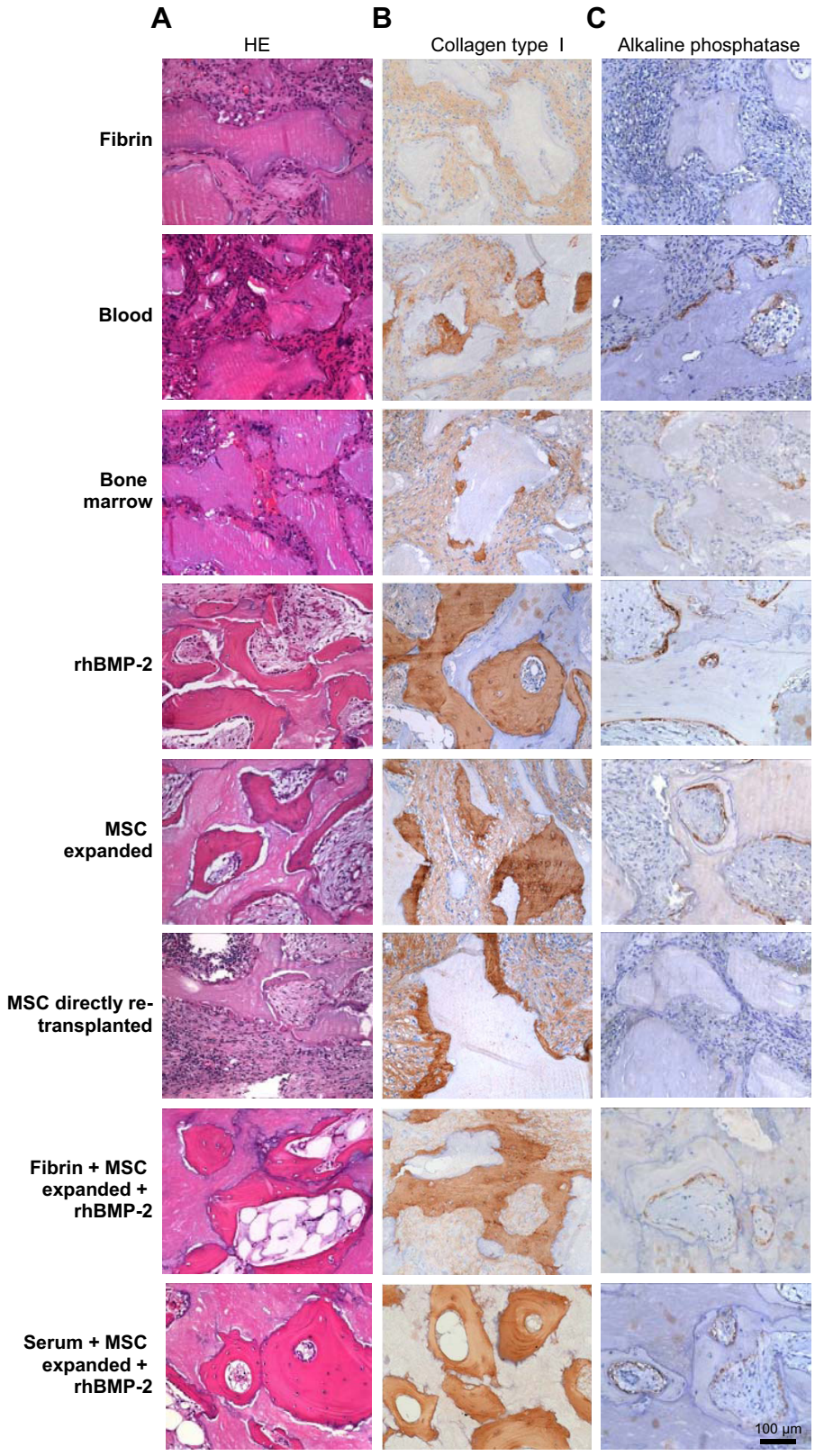

Figure 6 Histological overview of the explants.
Notes: For a histological overview, explants were stained with HE (**A**). For detection of newly formed bone tissue, we performed immunohistological staining against collagen type I (**B**), the main component of the organic bone matrix, and alkaline phosphatase (**C**), an enzyme synthesized by osteoblasts. Areas positive for collagen type I and alkaline phosphatase were obvious in all explants to some extent. Collagen type I marks the newly formed bone (brown color) which was found mainly near the bone substitute. Alkaline phosphatase (brown color) could be detected near the ossification zone next to osteoblasts synthesizing new bone tissue.
Abbreviations: MSC, mesenchymal stem cells; HE, hematoxylin-eosin; rhBMP-2, recombinant human bone morphogenetic protein 2.

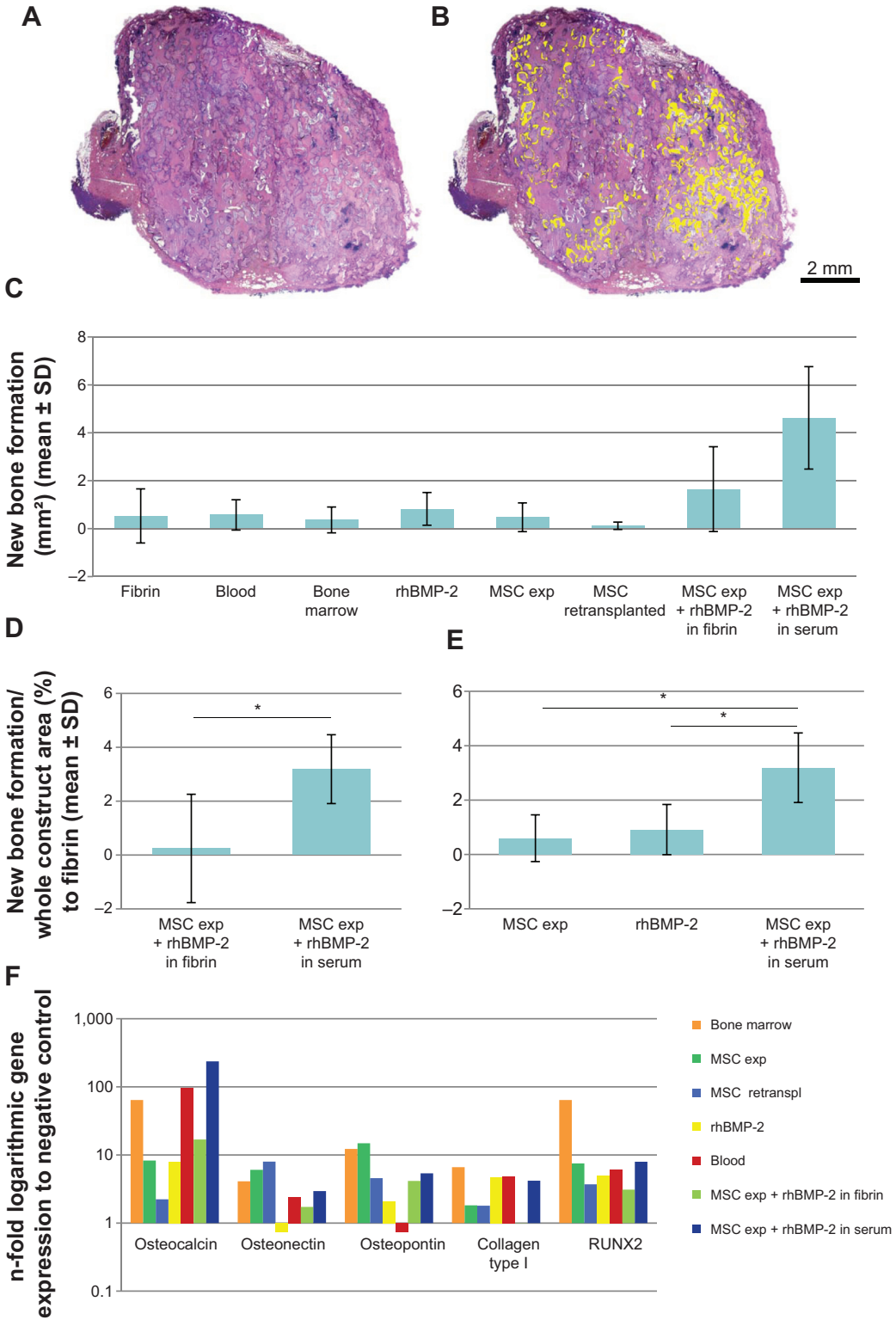

Figure 7 New bone formation.

Notes: (**A**, **B**) Bone formation was quantified semiautomatically using sections stained with hematoxylin-eosin. Single images at 25× magnification were assembled into one overview image. Newly formed bone was detected using a binary mask system. Bone tissue is marked in yellow. (**C**) The highest quantities of bone formation could be achieved in the booster groups combining rhBMP-2 and expanded MSC in the carrier material fibrin or autologous serum. (**D**) The booster group with rhBMP-2 and expanded MSC in autologous serum induced significantly more bone formation than the booster group in fibrin. (**E**) Combining expanded MSC and rhBMP-2 in autologous serum, bone formation was significantly enhanced compared with the groups with MSC and rhBMP-2 alone. (**F**) Quantitative real-time polymerase chain reaction analyses revealed upregulation of bone-specific genes, ie, osteocalcin, osteonectin, osteopontin, collagen type I and RUNX2, in nearly all groups compared with the control (fibrin). There were no statistically significant differences between the groups. *$P \leq 0.05$.

Abbreviations: exp, expanded; retranspl, retransplanted; MSC, mesenchymal stem cells; SD, standard deviation; rhBMP-2, recombinant human bone morphogenetic protein 2.

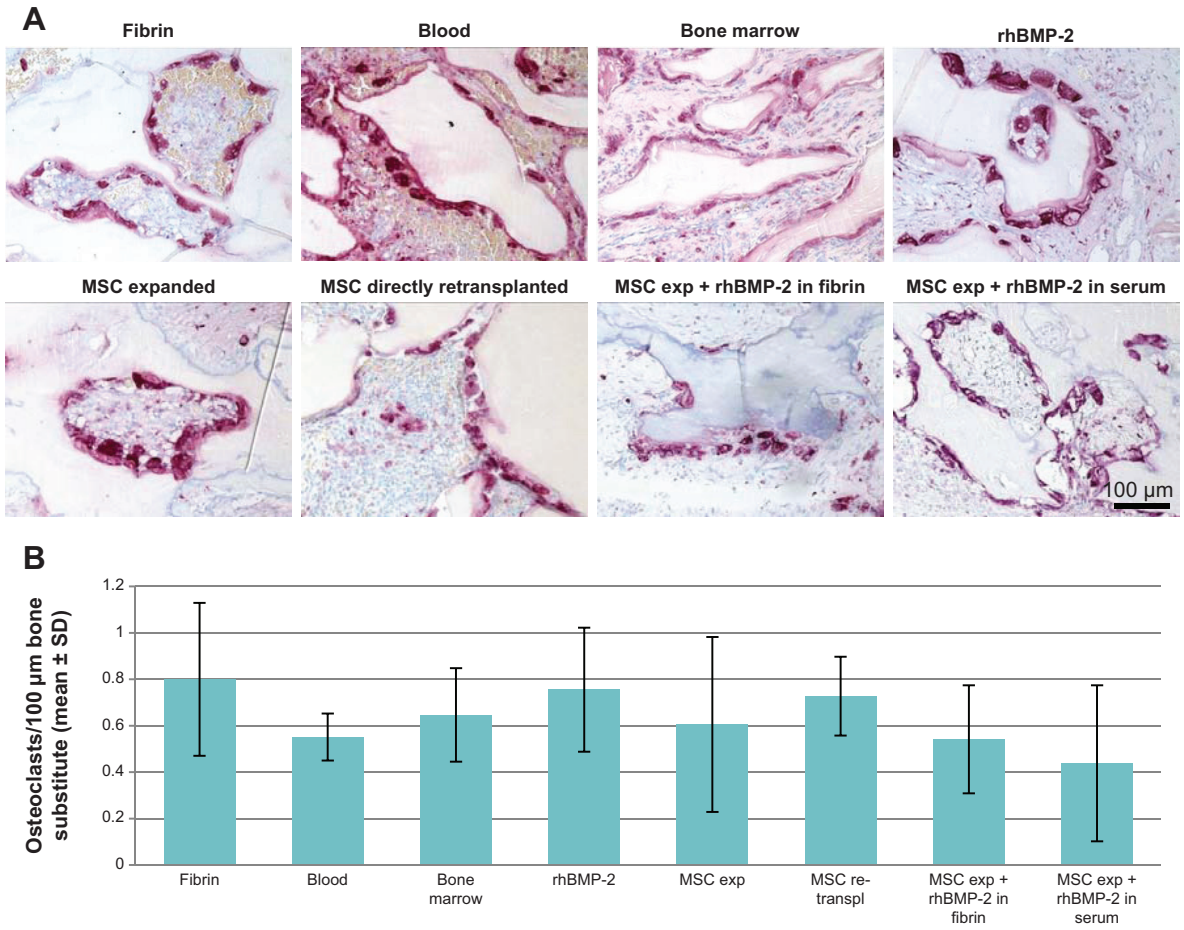

Figure 8 Osteoclastic activity in the explants.
Notes: (**A**) Sections from all experimental groups were stained with tartrate-resistant acid phosphatase to assess osteoclastic activity. Osteoclasts (stained in red) were mainly located at the surface of the bone substitute particles, showing a nearly equal distribution of osteoclastic activity over the constructs. (**B**) Osteoclasts were counted semiautomatically, with no significant differences found between the different experimental groups.
Abbreviations: exp, expanded; retranspl, retransplanted; MSC, mesenchymal stem cells; SD, standard deviation; rhBMP-2, recombinant human bone morphogenetic protein 2.

Behavior of directly retransplanted versus expanded MSC

Retrieval of cells from histological sections of the explanted constructs was possible because of DiI labeling of the MSC prior to implantation. Both directly retransplanted and expanded MSC could be detected in the explanted constructs. However, cells were distributed all over the areas with tissue ingrowth only in the group with expanded MSC. Directly retransplanted MSC could be identified in noticeably smaller numbers and only in some parts of the constructs (Figures 11 and 12).

To confirm proliferation and viability of the transplanted cells, staining with Ki67, a proliferation marker, was performed and apoptotic cells were detected by TUNEL assay. Proliferating cells were identified all over the constructs in areas with tissue ingrowth. Cells double-stained for Ki67 and DiI could be detected in the experimental groups with expanded MSC but not in the groups with directly retransplanted MSC (Figure 11). In all explants, only single apoptotic cells could be identified by TUNEL assay (Figure 12).

Discussion

In this study, a nano-HA bone substitute was implanted subcutaneously with various additives in a large animal model of the sheep. In the first part of the study, optimal cell carrier materials were evaluated (fibrin, cell culture medium, autologous serum) during an implantation period of 4 weeks. In addition, in the second part of the study, the bone substitute was soaked with different cell types (blood, bone marrow, MSC directly retransplanted and expanded) and the bone growth factor rhBMP-2, and implanted for 12 weeks. Finally, the best additives in parts 1 and 2 of the study were combined in part 3 (implantation period 12 weeks).

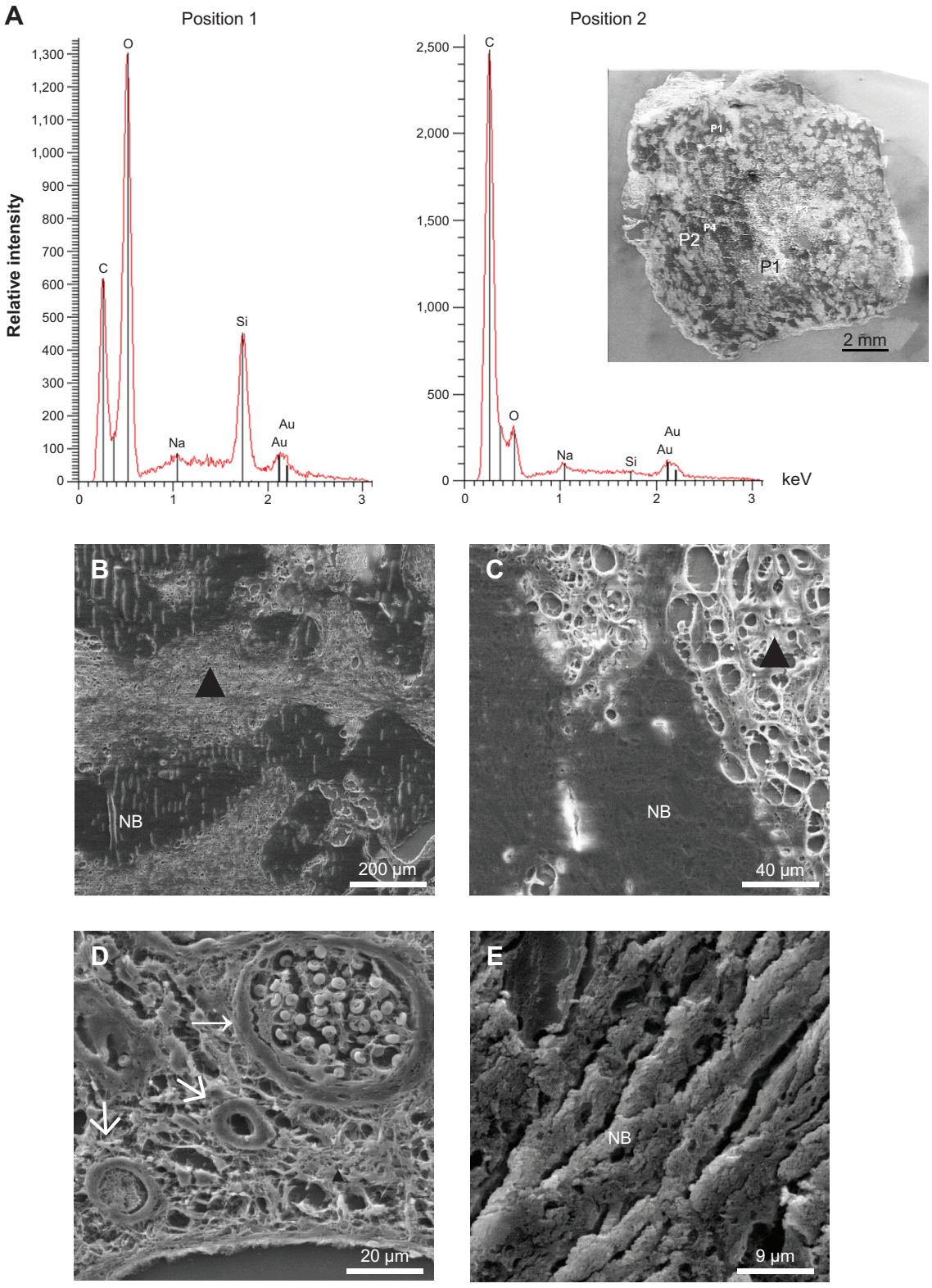

Figure 9 Scanning electron microscopy and energy dispersive x-ray spectroscopy.

Notes: (**A**) Scanning electron microscopy and energy dispersive x-ray spectroscopy were performed for slides from each experimental group to determine the elemental composition in the constructs. In each section, two to eight different positions concerning structure and shading were chosen for measurement. In areas with no or slight tissue ingrowth, relatively high levels of silicon and oxygen could be detected, reflecting the original composition of the bone substitute particles (position 1). However, in areas with high tissue ingrowth, high carbon and low silicon levels were found, indicating the change from an inorganic to an organic matrix (position 2). (**B**–**E**) Different magnifications of the explants are shown. The nanohydroxyapatite bone substitute particles are surrounded by connective tissue and blood vessels, particularly on the borders of the explants. In centrally located areas with less or no tissue ingrowth, remodeling of the bone substitute could not be induced. Bone substitute, ▲: tissue ingrowth, arrows: newly formed blood vessels. NB = NanoBone®.

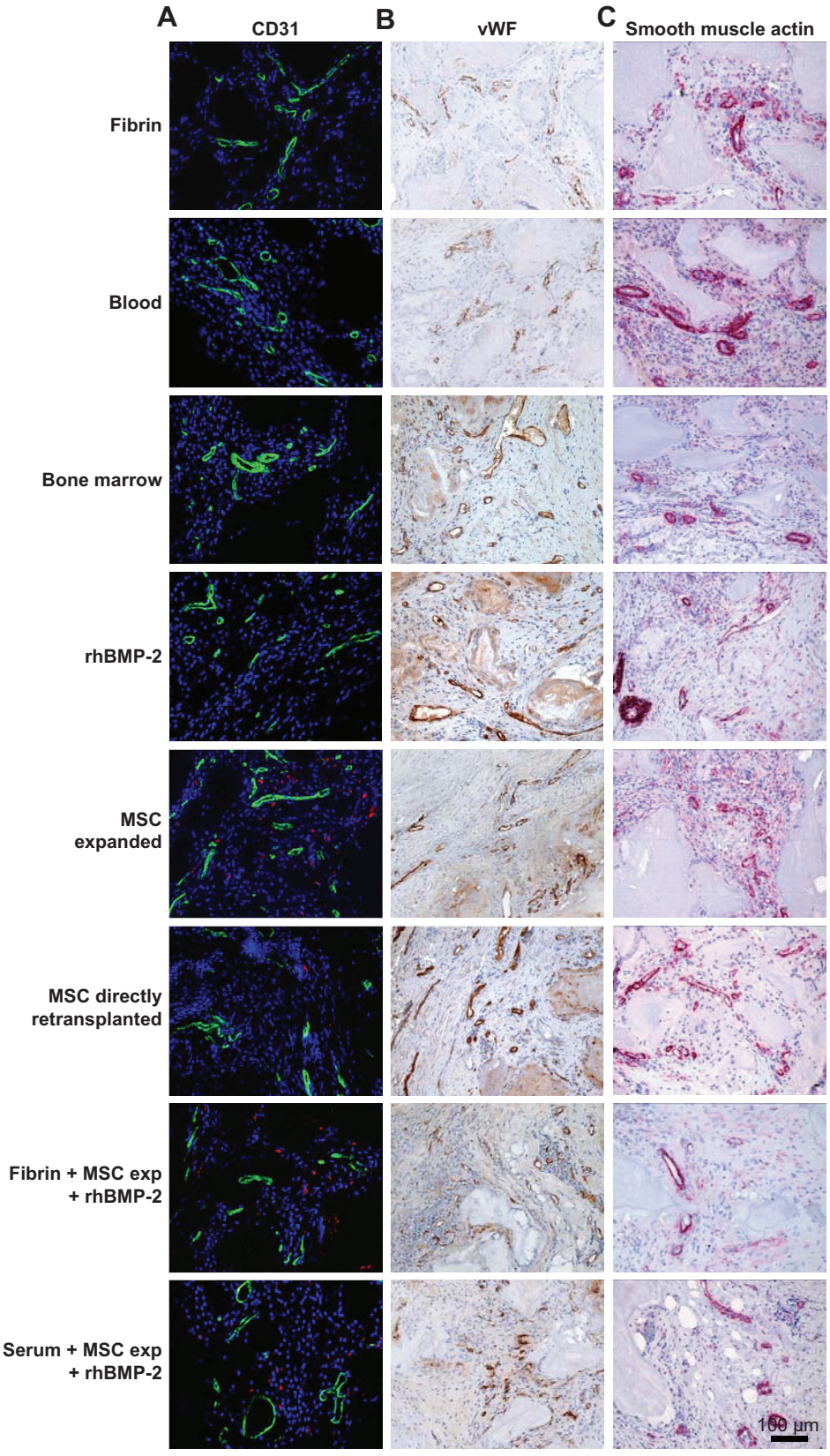

Figure 10 Vascularization of the explants.
Notes: All explants were stained for CD31 (**A**), vWF (**B**), and alpha smooth muscle actin (αSMA) (**C**) to examine vascularization. Newly formed vessels could be detected and were nearly equally distributed all over the constructs. However, some regions with no vessels were observed, consistent with areas of the construct with no tissue ingrowth.
Abbreviations: exp, expanded; MSC, mesenchymal stem cells; rhBMP-2, recombinant human bone morphogenetic protein 2; vWF, von Willebrand factor.

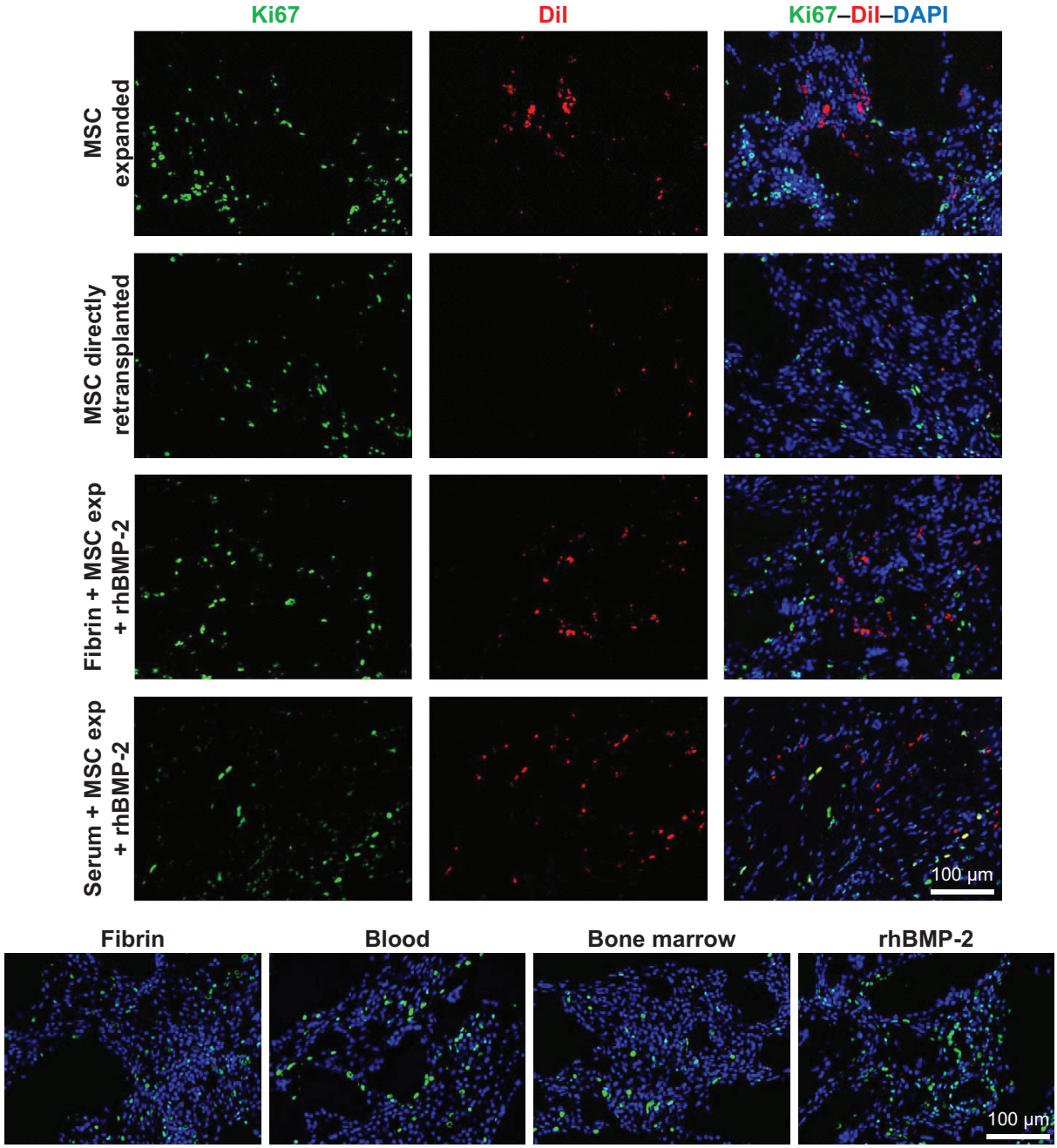

Figure 11 Proliferation of implanted cells.
Notes: Staining for the proliferation marker Ki67 was performed to demonstrate proliferation and viability of the transplanted cells. For retrieval of implanted MSC, cells were labeled using DiI before implantation. Proliferating cells were identified all over the constructs in areas with tissue ingrowth. Ki67 (green) and DiI (red) double-stained cells could be detected in the experimental groups with expanded MSC. Counterstaining was performed using DAPI (blue) staining.
Abbreviations: exp, expanded; MSC, mesenchymal stem cells; rhBMP-2, recombinant human bone morphogenetic protein 2; DAPI, 4′,6-diamidino-2′-phenylindole dihydrochloride; DiI, dioctadecyl-3,3,3′3′-tetramethylindocarbocyanine perchlorate.

Our results indicate that soaking the nano-HA bone substitute with autologous serum is superior to the clinically approved whole blood and the established cell carrier material, fibrin. Autologous serum in combination with expanded MSC and rhBMP-2 demonstrated the best results with regard to absorption of the scaffold, tissue ingrowth, vascularization, and newly formed bone within the explants.

Nanostructured bone substitute and its biocompatibility

The bone substitute is a nanostructured, fully synthetic bone substitute consisting of nanocrystalline HA embedded in a highly porous matrix of silica gel. The bone substitute is not a sintered ceramic, and is produced by what is known as the sol-gel process at a temperature lower than the sintering

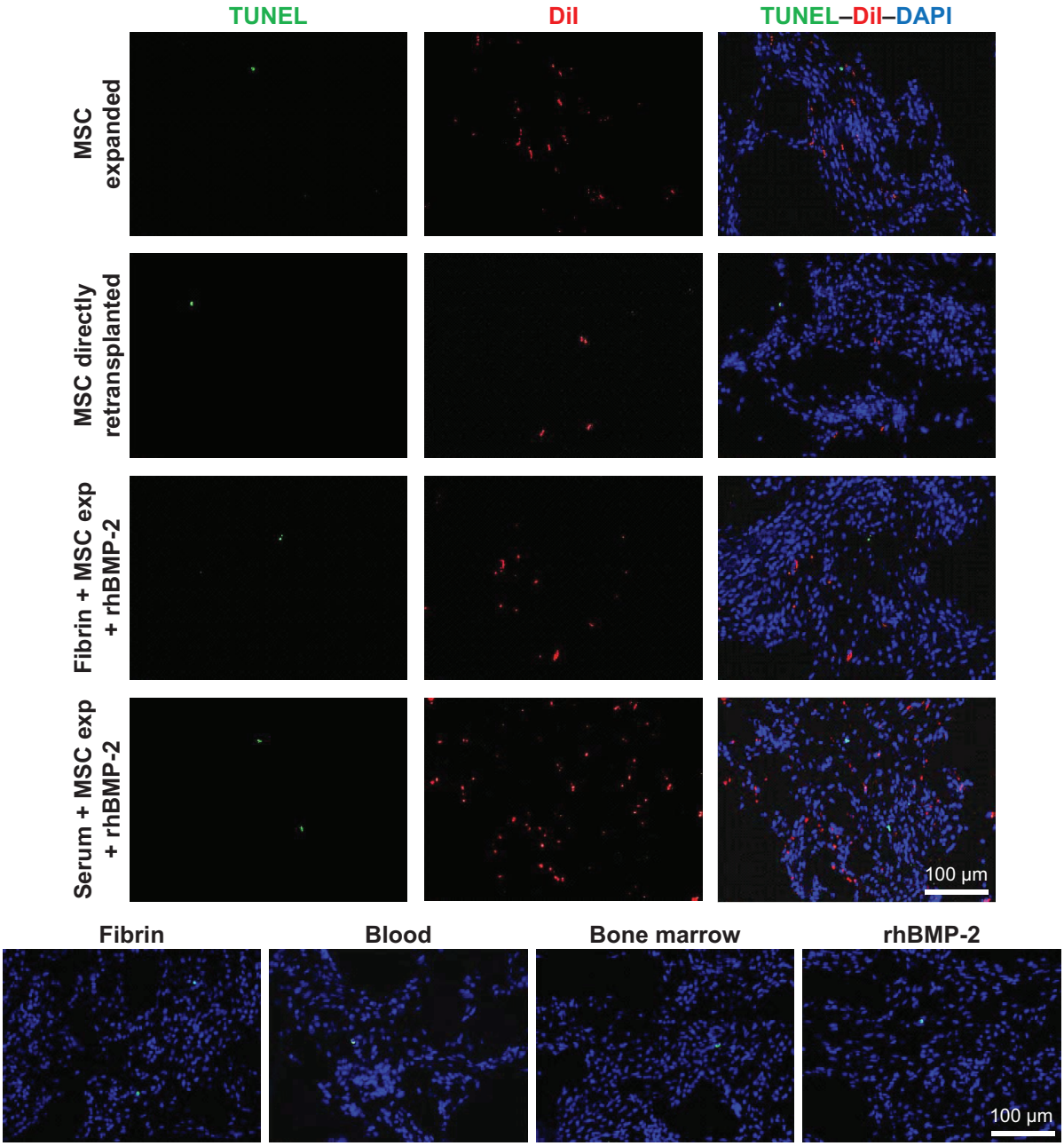

Figure 12 Apoptosis of implanted cells.
Notes: The TUNEL assay was performed to evaluate apoptosis in the constructs. For retrieval of implanted MSC, cells were stained with DiI (red) before implantation. In all explants, only single apoptotic cells (green staining) could be identified. Counterstaining was performed using DAPI (blue) staining.
Abbreviations: exp, expanded; MSC, mesenchymal stem cells; rhBMP-2, recombinant human bone morphogenetic protein 2; DAPI, 4′,6-diamidino-2′-phenylindole dihydrochloride; DiI, dioctadecyl-3,3,3′3′-tetramethylindocarbocyanine perchlorate; TUNEL, terminal deoxynucleotidyl transferase dUTP nick end labeling.

temperature of HA and silica. The crystallites are loosely packed and held together by SiO_2, leading to nanopores in the range of 10–20 nm.[24] In addition, micrometer and millimeter pores led to a high porosity of about 60% and to a very large internal surface (84 m^2/g) favoring the invasion of osteogenic cells and newly formed vessels.

Nevertheless, the nano-HA bone substitute has a high breaking strength of about 40 MPa. Results of animal experiments, preliminary clinical studies, and histological findings of bone biopsies after implantation suggest this bone substitute to be osteoconductive, osteoinductive, and a promoter of early bone remodeling.[13,15] The synthetic nanocrystalline HA is morphologically very similar to biological apatite in bone mineral. A variety of in vitro and in vivo experiments have shown that silicon-rich biomaterials are biocompatible and bioactive with osteoconductive characteristics. Previous work suggested that HA with incorporation of silicate ions significantly improved in vivo bioactivity compared with

conventional HA materials.[25] Another study demonstrated that a bone substitute comprised of nanocrystalline HA embedded in a silica matrix was successful in oral and maxillofacial surgery.[14] A previous study showed that the silica gel in the bone substitute is replaced by bone matrix glycoproteins with known functions in attraction, adhesion, and differentiation of bone cells as osteoblasts and osteoclasts.[25] Silica has an important impact on regulation of generation, mobilization, differentiation, and activation of osteoclast precursors. It has been established that a high silica content promotes rapid bone mineralization.[26] These findings indicate that this bone substitute could be an ideal material for the treatment of critical size defects.

The implants were well tolerated overall by the sheep. Only one sheep developed an infection, which is within the common range for this animal model. The good biocompatibility has been shown previously in in vivo studies and in clinical application.[24,27]

Optimal cell carrier material

For evaluation of an optimal cell carrier material, the bone substitute was implanted in combination with expanded or directly retransplanted MSC and fibrin, cell culture medium, or autologous serum. An important aspect of this study was the bone formation capacity of the different groups. Hardly any bone formation was found in explants with directly retransplanted MSC. Therefore, analysis of the first part of the study was reduced to experimental groups with expanded MSC. Cell culture medium and autologous serum proved to be superior to fibrin with regard to bone formation capacity, tissue ingrowth, and degradation of the bone substitute. In constructs with cell culture medium and autologous serum, more TRAP-positive cells could be identified when compared with fibrin. This may be in concordance with reduced vascularization and absorption of the bone substitute in the fibrin group. The expression of osteogenic genes did not demonstrate a significant difference between the experimental groups.

All these findings can probably be explained by the higher viscosity of fibrin, which is not able to penetrate the block material as good as the more liquid autologous serum or cell culture medium. Irregular soaking of the fibrin sealant may be the reason for the inconsistent bone formation and high standard deviation in the fibrin groups. Positive proliferative and angiogenic effects have been described by other groups, and should have made fibrin an ideal carrier medium for MSC for bone tissue engineering purposes. However, in this study, autologous serum and cell culture medium seemed to be more promising.[28,29] An advantage of autologous serum is that it contains a broad range of growth factors and cytokines. It has been shown that autologous serum has a positive influence on MSC behavior.[30] For positively charged molecules in particular, it is possible to stick to the negatively charged surface by SiO groups of the bone substitute and therefore promote the remodeling process.[31] Fibrin could cover the bone substitute surface and therefore mask the SiO groups, so that the matrix change and induction of bone formation could not take place. In addition, use of autologous serum is not associated with as many regulatory issues as using serum or fibrin of foreign species.[32] Due to the range of positive aspects of autologous serum and the similar results with cell culture medium, we finally decided to use autologous serum in the following part of the study.

Degradation, absorption, and matrix change of bone substitute

As cell sources, blood, bone marrow, directly retransplanted and expanded MSC were implanted in combination with the bone substitute. Expanded MSC proved to be the optimal cell source with regard to adequate absorption and degradation of the bone substitute, good tissue ingrowth, bone formation capacity, and cell proliferation.

A crucial aspect of bone regeneration using bone substitutes is absorption of the bone substitute and simultaneous formation of new bone.[33] In this study, shrinkage of the whole constructs, degradation of the scaffold, and the tissue ingrowth area were analyzed. The largest tissue ingrowth areas and complete vascularization could be achieved in groups with blood and bone marrow, and finally in the "booster group" combining expanded MSC and rhBMP-2 in serum.

Tissue ingrowth areas in the other experimental groups covered about 80% after 12 weeks. However, highly significant shrinkage of the experimental groups with blood and bone marrow was obvious when compared with other cell sources or combination with rhBMP-2, as shown in Figure 5G. Other researchers working with nano-HA granules or blocks soaked in blood have observed absorption of the bone substitute without adequate new bone formation.[25,34]

In the 12-week group, about 50% of the bone substitute particles were degraded. Other groups observed degradation and complete absorption under the same circumstances because of the high porosity and loosely packed HA structure of the bone substitute.[12,35] Compared with other bone substitutes, NanoBone® was degraded in a faster manner, which could avoid the risk of residual bone substitute material and an inflammatory response.[27,36]

TRAP-positive cells could always be detected without significant differences between the groups. After 12 weeks, significantly more TRAP-positive cells were counted than after 4 weeks. The appearance of TRAP-positive cells can be interpreted as a sign of early bone formation, as hypothesized by others.[25] However, the coexistence of TRAP-positive and osteoblastic cells and the absence of further inflammatory cells suggests the start of remodeling of the bone substitute rather than an inflammatory process. Götz et al explain the existence of TRAP-positive cells by the high content of osteocalcin and osteopontin on the surface of the bone substitute, stimulating osteoclast adhesion and differentiation.[13] More TRAP-positive cells were counted in the groups with less bone formation, possibly due to less free nano-HA bone substitute surface available for osteoclastic activity because of more newly formed bone near the bone substitute surface.

Representative sections were examined by electron microscopy to analyze the matrix change from an inorganic composition with high levels of silicon and oxygen to an organic composition with high levels of carbon. In some areas without any tissue ingrowth, relatively high amounts of inorganic matrix could be detected, representing the original bone substitute matrix. In contrast, in well vascularized areas, high amounts of carbon and low levels of silicon could be demonstrated. As described in previous studies,[13,15,23,31] a matrix change could be detected particularly near the surface of the bone substitute and only in well vascularized areas.[25] In our constructs, a matrix change was visible in all experimental groups and therefore paves the way for further degradation of the nano-HA bone substitute by osteoclasts and new bone formation.

New bone formation depending on implanted cells and carrier material

Areas positive for collagen type I and alkaline phosphatase could be detected in all constructs to varying degrees, demonstrating successful bone formation using the bone substitute in combination with different additives.

The nano-HA bone substitute is clinically approved, soaked with whole blood. There are several animal and clinical studies demonstrating that this strategy leads to a matrix change in the bone substitute and finally to formation of new bone.[27,34] Taking whole blood is a simple and rapid method for clinical application. In our study constructs soaked with whole blood, high interindividual variance concerning bone formation was obvious. In addition, bone formation remained very low compared with previous bone substitute studies. However, it has to be kept in mind that the present experiment involves induction of ectopic (that means in abnormal sites) bone formation in subcutis. Dietze et al emphasize that contact between the nano-HA bone substitute and well vascularized bone is essential for successful therapy.[37] For this reason, ectopic bone formation, needed for our tissue engineering purposes, is not possible using the bone substitute solely soaked with whole blood.

Differing interindividual results were observed in the group with bone marrow. Some sheep had high yields of bone formation, whereas some showed only early bone formation. This could be due to the heterogeneous cell population and often low numbers of MSC located in the bone marrow.[38] In addition, growth factor and cytokine concentrations are known to be very variable.[39,40] The expected benefit of endothelial progenitor cells and angiogenic growth factors, as described by other groups,[41–46] could not be observed.[47]

One strategy to improve these results is to concentrate the bone marrow cell fraction, which in the present study involved directly retransplanted MSC. However, even when working with concentrated cell suspensions, varying cell numbers are yielded, which can make even robust results questionable.[48] Expanded MSC have been used in a wide range of studies, both for bone tissue purposes and in other fields of regenerative medicine.[49,50] MSC are expected to be the ideal cell population because of their good differentiation capacity as well as their secretion of a wide range of regulatory cytokines and their good influence as anti-inflammatory and immunosuppressive agents.[51] After 12 weeks, expanded MSC did not induce significantly more bone formation than directly retransplanted MSC. However, after 4 weeks, expanded MSC clearly showed an earlier and faster potential for new bone formation. Moreover, in constructs with directly retransplanted MSC, less labeled MSC could be found than in constructs with expanded MSC. This could possibly be due to the higher cell numbers achieved after expansion and the variable and low numbers of stem cells in the concentrated directly retransplanted MSC, which could not be determined before implantation.

RhBMP-2 was used as a bone growth factor, inducing a high rate of bone formation in the constructs alone and in combination with expanded MSC. Because of its well known osteogenic capacity, BMP-2 has been approved for clinical application and a huge range of experimental studies have made use of it.[52] In a preliminary study, two concentrations of rhBMP-2 were tested in combination with the bone substitute, showing an advantage of 60 μg/mL when compared

with 12.5 µg/mL (data not shown). The BMP concentration needed for healing of bone defects is unknown so far.[53] The concentration depends on the species, the carrier material, and the defect itself.[52,54] Side effects of high concentrations could possibly lead to ectopic bone formation and an increase in osteoclastic activity. In our study, osteoclastic activity was comparable in all constructs from the 12-week group, and bone formation in the tissue around the implants could not be observed.

BMP-2 should be used in a carrier medium that ensures its slow release over time. Fibrin was used for that purpose in several previous studies, and seems to be ideal for slow growth factor release. In addition, it is absorbable and supports angiogenic ingrowth.[55,56] In this study, soaking the scaffolds with fibrin resulted in inferior results when compared with autologous serum and cell culture medium, possibly due to the special nanostructured architecture. Comparison of the two combination groups with expanded MSC and rhBMP-2 in fibrin and serum demonstrated that fibrin is not crucial for the delivery of the growth factor BMP-2 over time. We could clearly show that addition of BMP-2 to serum markedly increases the capacity for bone formation while always using the same batch of serum, so at least intratest validity and reproducibility were ensured in this study.

HA is a calcium phosphate ($Ca_5(PO_4)_3OH$), which represents 55% of the weight of bone in vertebrates. Silicon, an essential trace element, plays an active role in human bone mineralization and calcification, and was demonstrated to be pivotal in formation of connective tissue and stimulation of osteoblast proliferation.[25,26] The bone substitute used in this study has been made of both HA and silica, which is achieved through specific sol-gel techniques. After heterotopic transplantation of this bone substitute, there is a change of the inorganic silica gel matrix into organic host compounds.[25] By soaking the bone substitute with growth factors, the protein is incorporated into the scaffold prior to the matrix change. The kinetics of the initial matrix change of the implanted biomaterial are enhanced by this procedure. The protein is released into the extracellular environment during the following matrix change and degradation of the bone substitute, supporting bone growth.

Quantitative real-time PCR analyses revealed upregulation of osteocalcin, osteonectin, osteopontin, collagen type I, and RUNX2 in nearly all groups when compared with the control (bone substitute with fibrin). No statistically significant differences between the experimental groups could be determined. However, high standard deviations were observed. The upregulation of osteogenic markers in all the bone substitute groups indicates good osteogenic and osteoinductive properties of the nano-HA bone substitute, as described previously.[13] It should be noted that the areas in which bone formation and remodeling of the bone substitute take place were not equally distributed over the constructs. Only a small part of the explants was analyzed for molecular biology, probably leading to use of non-representative samples from the experimental groups and resulting in high standard deviations.

Conclusion

A nanostructured clinically approved bone substitute material was evaluated in this study, soaked with different carrier materials, and implanted in a large animal model in combination with different cells and the bone growth factor rhBMP-2. Autologous serum improves tissue ingrowth of the nano-HA bone substitute and leads to earlier and more rapid bone formation compared with fibrin. Because of its low viscosity, autologous serum is ideal for penetration of the nanostructured bone substitute and can induce early matrix change by delivery of a wide range of autologous growth factors and cytokines. Osteogenic cells and rhBMP-2 could therefore evenly distribute into the bone substitute, with degradation and simultaneous bone formation within the nano-HA bone substitute being stimulated.

Combining expanded MSC with rhBMP-2 in autologous serum leads to a high yield of bone formation and is superior to the clinically approved procedure where the bone substitute is soaking in whole blood. In the next step, these results should be transferred to the sheep arteriovenous loop model to engineer axially vascularized primary stable bone replacement of a clinically relevant size.

Acknowledgments

We would like to thank Stefan Fleischer, Marina Milde, and Ilse Arnold-Herberth for their excellent technical support. This work contains parts of the doctoral theses of A Weigand and G Deschler. This study was funded by the ELAN Fonds für Forschung und Lehre, University of Erlangen-Nürnberg, Erlangen, Germany; the Baxter Innovations GmbH, Vienna, Austria; the Staedtler Foundation, University of Erlangen-Nürnberg, Erlangen, Germany; the Forschungsstiftung Medizin Erlangen, University of Erlangen-Nürnberg, Erlangen, Germany; and the Xue Hong and Hans Georg Geis Foundation. We acknowledge support by Deutsche Forschungsgemeinschaft and Friedrich-Alexander-Universität Erlangen-Nürnberg as part of the Open Access Publishing funding program.

Disclosure

One of the authors (TG) was involved in the development of the bone substitute material. He is executive director of Artoss GmbH, the distributor of NanoBone®. He was involved in the design of the study. All other authors confirm that they have no conflicts of interest in this work.

References

1. Horch RE, Kneser U, Polykandriotis E, Schmidt VJ, Sun J, Arkudas A. Tissue engineering and regenerative medicine – where do we stand? *J Cell Mol Med.* 2012;16(6):1157–1165.
2. Horch RE, Boos AM, Quan Y, et al. Cancer research by means of tissue engineering – is there a rationale? *J Cell Mol Med.* 2013;17(10):1197–1206.
3. Ma J1, Both SK, Yang F, Cui FZ, Pan J, Meijer GJ, Jansen JA, van den Beucken JJ. Concise review: cell-based strategies in bone tissue engineering and regenerative medicine. *Stem Cells Transl Med.* 2014 Jan;3(1):98–107. doi: 10.5966/sctm.2013-0126. Epub 2013 Dec 3.
4. Dawson JI1, Kanczler J, Tare R, Kassem M, Oreffo RO. Concise review: bridging the gap: bone regeneration using skeletal stem cell-based strategies - where are we now? *Stem Cells*. 2014;32(1):35–44. doi: 10.1002/stem.1559.
5. Arvidson K, Abdallah BM, Applegate LA, et al. Bone regeneration and stem cells. *J Cell Mol Med.* 2011;15(4):718–746.
6. Barrere F, van Blitterswijk CA, de Groot K. Bone regeneration: molecular and cellular interactions with calcium phosphate ceramics. *Int J Nanomedicine.* 2006;1(3):317–332.
7. Hing KA, Revell PA, Smith N, Buckland T. Effect of silicon level on rate, quality and progression of bone healing within silicate-substituted porous hydroxyapatite scaffolds. *Biomaterials.* 2006;27(29):5014–5026.
8. Xu S, Lin K, Wang Z, et al. Reconstruction of calvarial defect of rabbits using porous calcium silicate bioactive ceramics. *Biomaterials.* 2008;29(17):2588–2596.
9. Patel N, Brooks RA, Clarke MT, et al. In vivo assessment of hydroxyapatite and silicate-substituted hydroxyapatite granules using an ovine defect model. *J Mater Sci Mater Med.* 2005;16(5):429–440.
10. Huang DM, Chung TH, Hung Y, et al. Internalization of mesoporous silica nanoparticles induces transient but not sufficient osteogenic signals in human mesenchymal stem cells. *Toxicol Appl Pharmacol.* 2008;231(2):208–215.
11. Xu JL, Khor KA. Chemical analysis of silica doped hydroxyapatite biomaterials consolidated by a spark plasma sintering method. *J Inorg Biochem.* 2007;101(2):187–195.
12. Gerike W, Bienengraber V, Henkel KO, et al. The manufacture of synthetic non-sintered and degradable bone grafting substitutes. *Folia Morphol (Warsz).* 2006;65(1):54–55.
13. Gotz W, Gerber T, Michel B, Lossdorfer S, Henkel KO, Heinemann F. Immunohistochemical characterization of nanocrystalline hydroxyapatite silica gel (NanoBone(r)) osteogenesis: a study on biopsies from human jaws. *Clin Oral Implants Res.* 2008;19(10):1016–1026.
14. Heinemann F, Mundt T, Biffar R, Gedrange T, Goetz W. A 3-year clinical and radiographic study of implants placed simultaneously with maxillary sinus floor augmentations using a new nanocrystalline hydroxyapatite. *J Physiol Pharmacol.* 2009;60 Suppl 8:91–97.
15. Henkel KO, Gerber T, Lenz S, Gundlach KK, Bienengraber V. Macroscopical, histological, and morphometric studies of porous bone-replacement materials in minipigs 8 months after implantation. *Oral Surg Oral Med Oral Pathol Oral Radiol Endod.* 2006;102(5):606–613.
16. Rath SN, Strobel LA, Arkudas A, et al. Osteoinduction and survival of osteoblasts and bone-marrow stromal cells in 3D biphasic calcium phosphate scaffolds under static and dynamic culture conditions. *J Cell Mol Med.* 2012;16(10):2350–2361.
17. Jones E, Yang X. Mesenchymal stem cells and bone regeneration: current status. *Injury.* 2011;42(6):562–568.
18. Cancedda R, Bianchi G, Derubeis A, Quarto R. Cell therapy for bone disease: a review of current status. *Stem Cells.* 2003;21(5):610–619.
19. Chen HT, Lee MJ, Chen CH, et al. Proliferation and differentiation potential of human adipose-derived mesenchymal stem cells isolated from elderly patients with osteoporotic fractures. *J Cell Mol Med.* 2012;16(3):582–593.
20. Garrison KR, Shemilt I, Donell S, et al. Bone morphogenetic protein (BMP) for fracture healing in adults. *Cochrane Database Syst Rev.* 2010;6:CD006950.
21. Pneumaticos SG, Triantafyllopoulos GK, Basdra EK, Papavassiliou AG. Segmental bone defects: from cellular and molecular pathways to the development of novel biological treatments. *J Cell Mol Med.* 2010;14(11):2561–2569.
22. Govender S, Csimma C, Genant HK, et al. Recombinant human bone morphogenetic protein-2 for treatment of open tibial fractures: a prospective, controlled, randomized study of four hundred and fifty patients. *J Bone Joint Surg Am.* 2002;84A(12):2123–2134.
23. Boos AM, Loew JS, Weigand A, et al. Engineering axially vascularized bone in the sheep arteriovenous-loop model. *J Tissue Eng Regen Med.* 2013;7(8):654–664.
24. Abshagen K, Schrodi I, Gerber T, Vollmar B. In vivo analysis of biocompatibility and vascularization of the synthetic bone grafting substitute NanoBone. *J Biomed Mater Res A.* 2009;91(2):557–566.
25. Xu W, Holzhuter G, Sorg H, et al. Early matrix change of a nanostructured bone grafting substitute in the rat. *J Biomed Mater Res B Appl Biomater.* 2009;91(2):692–699.
26. Jugdaohsingh R. Silicon and bone health. *J Nutr Health Aging.* 2007;11(2):99–110.
27. Bienengraber V, Gerber T, Henkel KO, Bayerlein T, Proff P, Gedrange T. The clinical application of a new synthetic bone grafting material in oral and maxillofacial surgery. *Folia Morphol (Warsz).* 2006;65(1):84–88.
28. Lee OK. Fibrin glue as a vehicle for mesenchymal stem cell delivery in bone regeneration. *J Chin Med Assoc.* 2008;71(2):59–61.
29. Rajangam T, An SS. Fibrinogen and fibrin based micro and nano scaffolds incorporated with drugs, proteins, cells and genes for therapeutic biomedical applications. *Int J Nanomedicine.* 2013;8:3641–3662.
30. Kobayashi T, Watanabe H, Yanagawa T, et al. Motility and growth of human bone-marrow mesenchymal stem cells during ex vivo expansion in autologous serum. *J Bone Joint Surg Br.* 2005;87(10):1426–1433.
31. Gerber T, Holzhüter G, Götz W, Bienengräber V, Henkel K-O, Rumpel E. Nanostructuring of biomaterials – a pathway to bone grafting substitute. *Eur J Trauma.* 2006;32(2):132–140.
32. Choi J, Chung JH, Kwon GY, Kim KW, Kim S, Chang H. Effectiveness of autologous serum as an alternative to fetal bovine serum in adipose-derived stem cell engineering. *Cell Tissue Bank.* 2013;14(3):413–422.
33. Kolk A, Handschel J, Drescher W, et al. Current trends and future perspectives of bone substitute materials – from space holders to innovative biomaterials. *J Craniomaxillofac Surg.* 2012;40(8):706–718.
34. Kirchhoff M, Lenz S, Henkel KO, et al. Lateral augmentation of the mandible in minipigs with a synthetic nanostructured hydroxyapatite block. *J Biomed Mater Res B Appl Biomater.* 2011;96(2):342–350.
35. Rumpel E, Wolf E, Kauschke E, et al. The biodegradation of hydroxyapatite bone graft substitutes in vivo. *Folia Morphol (Warsz).* 2006;65(1):43–48.
36. Liu Y, Wang G, Cai Y, et al. In vitro effects of nanophase hydroxyapatite particles on proliferation and osteogenic differentiation of bone marrow-derived mesenchymal stem cells. *J Biomed Mater Res A.* 2009;90(4):1083–1091.
37. Dietze S, Bayerlein T, Proff P, Hoffmann A, Gedrange T. The ultrastructure and processing properties of Straumann bone ceramic and nanobone. *Folia Morphol (Warsz).* 2006;65(1):63–65.

38. Filip S, Mokry J, Vavrova J, et al. The peripheral chimerism of bone marrow-derived stem cells after transplantation: regeneration of gastrointestinal tissues in lethally irradiated mice. *J Cell Mol Med.* 2014;18(5):832–843.
39. Meyer U, Wiesmann HP, Berr K, Kubler NR, Handschel J. Cell-based bone reconstruction therapies – principles of clinical approaches. *Int J Oral Maxillofac Implants.* 2006;21(6):899–906.
40. Hernigou P, Homma Y. Tissue bioengineering in orthopedics. *Clin Cases Miner Bone Metab.* 2012;9(1):21–23.
41. Masuda H, Asahara T. Post-natal endothelial progenitor cells for neovascularization in tissue regeneration. *Cardiovasc Res*. 2003;58(2): 390–398.
42. Geuze RE, et al. Influence of endothelial progenitor cells and platelet gel on tissueengineered bone ectopically in goats. *Tissue Eng Part A*. 2009;15(11):3669–3677.
43. Seebach C, et al. Endothelial progenitor cells improve directly and indirectly early vascularization of mesenchymal stem cell-driven bone regeneration in a critical bone defect in rats. *Cell Transplant*. 2012;21(8):1667–1677.
44. Zigdon-Giladi H, et al. Mesenchymal Stem Cells and Endothelial Progenitor Cells Stimulate Bone Regeneration and Mineral Density. *J Periodontol*, 2013.
45. Aguirre A, Planell JA, Engel E. Dynamics of bone marrow-derived endothelial progenitor cell/mesenchymal stem cell interaction in co-culture and its implications in angiogenesis. *Biochem Biophys Res Commun*. 2010;400(2):284–291.
46. Henrich D, et al, Simultaneous cultivation of human endothelial-like differentiated precursor cells and human marrow stromal cells on beta-tricalcium phosphate. *Tissue Eng Part C Methods*. 2009;15(4):551–560.
47. Tateishi-Yuyama E, Matsubara H, Murohara T, et al. Therapeutic angiogenesis for patients with limb ischaemia by autologous transplantation of bone-marrow cells: a pilot study and a randomised controlled trial. *Lancet.* 2002;360(9331):427–435.
48. Zhong W, Sumita Y, Ohba S, et al. In vivo comparison of the bone regeneration capability of human bone marrow concentrates vs platelet-rich plasma. *PLoS One.* 2012;7(7):e40833.
49. Choudhery MS, Khan M, Mahmood R, et al. Mesenchymal stem cells conditioned with glucose depletion augments their ability to repair-infarcted myocardium. *J Cell Mol Med.* 2012;16(10):2518–2529.
50. Song L, Xu J, Qu J, et al. A therapeutic role for mesenchymal stem cells in acute lung injury independent of hypoxia-induced mitogenic factor. *J Cell Mol Med.* 2012;16(2):376–385.
51. Porada CD, Almeida-Porada G. Mesenchymal stem cells as therapeutics and vehicles for gene and drug delivery. *Adv Drug Deliv Rev.* 2010;62(12):1156–1166.
52. Lo KW, Ulery BD, Ashe KM, Laurencin CT. Studies of bone morphogenetic protein-based surgical repair. *Adv Drug Deliv Rev.* 2012;64(12):1277–1291.
53. Salgado AJ, Coutinho OP, Reis RL. Bone tissue engineering: state of the art and future trends. *Macromol Biosci.* 2004;4(8):743–765.
54. Cancedda R, Giannoni P, Mastrogiacomo M. A tissue engineering approach to bone repair in large animal models and in clinical practice. *Biomaterials.* 2007;28(29):4240–4250.
55. Schutzenberger S, Schultz A, Hausner T, et al. The optimal carrier for BMP-2: a comparison of collagen versus fibrin matrix. *Arch Orthop Trauma Surg.* 2012;132(9):1363–1370.
56. Arkudas A, Pryymachuk G, Hoereth T, et al. Composition of fibrin glues significantly influences axial vascularization and degradation in isolation chamber model. *Blood Coagul Fibrinolysis.* 2012;23(5):419–427.